

**An-Najah National University**

**Faculty of Graduate Studies**

**The Electronic Band pStructure of Graphene and  
Carbon Nanotubes**

**By**

**Asmahan Anan Sulaiman Tiryaki**

**Supervisor**

**Prof. Mohammad ELSAID**

**Co-Supervisor**

**Dr. Musa ELHASAN**

**This Thesis is submitted in Partial Fulfillment of Requirements for the  
Degree of Master of Physical Sciences, Faculty of Graduate Studies,  
An-Najah National University Nablus, Palestine.**

**2013**

**The Electronic Band Structure of Graphene and Carbon  
Nanotubes**

By

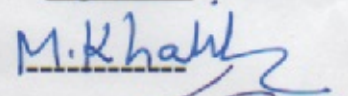
**Asmahan Anan Sulaiman Tiryaki**

**This Thesis was defended successfully on 11/4/2013 and approved  
by:**

**Defense Committee Members**

**Signature**

**- Prof.Mohammad Al-Said (Supervisor)**

  
-----

**- Dr. Musa Al-Hasan (co-supervisor)**

  
-----

**- Dr.Abdel-Rahman M.Abu-Labdeh (External Examiner)**

  
-----

**- Dr. Khaled Ilaiwi (Internal Examiner)**

  
-----

## **Dedication**

This thesis is dedicated to my father and my mother for their endless love, support and encouragement, to my brothers, sisters, friends and my family with love and respect.

## **Acknowledgements**

I am very pleased to express my deep gratitude to my supervisor Dr. Mohammad El-Said and co-supervisor Dr. Musa El-Hasan for their supervision, guidance and insightful suggestions.

Special thank is addressed to the student Ayham Shaer for helping me in using Mathematica.

My sincere thanks go to my lovely family and friends for their unlimited support.

## الإقرار

أنا الموقعة أدناه مقدمة الرسالة التي تحمل العنوان :

### **The Electronic Band Structure of Graphene and Carbon Nanotubes**

#### التركيب الإلكتروني للجرافين وأنابيب الكربون النانوية

أقر بأن ما اشتملت عليه هذه الرسالة إنما هي نتاج جهدي الخاص باستثناء ما تمت الإشارة إليه حيثما ورد. وأن هذه الرسالة ككل أو أي جزء منها لم يقدم من قبل لنيل أية درجة علمية لدى أية مؤسسة تعليمية أو بحثية أخرى.

### **Declaration**

The work provided in this thesis, unless otherwise referenced, is the researcher's own work, and has not been submitted elsewhere for any other degree or qualification.

**Student's name:**

اسم الطالب:

**Signature:**

التوقيع:

**Date:**

التاريخ:

## Table of contents

No.	Content	Page
	Dedication	iii
	Acknowledgements	iv
	Declaration	v
	List of Abbreviations	x
	List of Figures	viii
	Abstract	xi
	<b>Chapter One: Introduction</b>	<b>1</b>
1.1	Research Objectives	8
1.2	Previous Studies	8
1.3	Method of Calculations	12
	<b>Chapter Two: Theory</b>	<b>14</b>
2.1	Direct Lattice Structure of Graphene	15
2.2	The Reciprocal Lattice of Graphene	17
2.3	Carbon Nanotubes	18
2.4	Graphene Rolling Up	22
2.5	Electronic Band Structure of Graphene	25
2.5.1	Tight Binding Approximation	26
2.6	The Conical Shape of Graphene Dispersion Near The Dirac Points	32
2.7	Massless Dirac Particles	34
2.8	Band Structure of Carbon Nanotubes	36
2.9	Semiconducting Gap For Zigzag Carbon Nanotubes	37
2.10	Density of States (DOS)	38
2.10.1	Density of States of Graphene	38
2.10.2	Density of States of Zigzag Carbon Nanotubes	39
	<b>Chapter Three: Results and Discussions</b>	<b>42</b>
3.1	The Energy Dispersion Relation of Graphene	43
3.1.1	The Dispersion Relation as Function of $k_x$ and $k_y$	43
3.1.2	The Dispersion Relation as Function of $k_y$	44
3.2	The Dispersion Relation for the Zigzag CNTs	45
3.3	Semi Conducting Gap for Zigzag CNTs	49
3.4	The Density of States (DOS)	51
3.4.1	Density of States of Graphene	51
3.4.2	The DOS of Zigzag CNT	53
	<b>Chapter Four: Conclusion</b>	<b>56</b>
	References	60

	Appendix	65
	المخلص	ب

## List of Figures

No.	Figure	Page
1.1	Graphene as the source of three different nanomaterial systems.	5
1.2	The band structure of graphene near the Dirac point's $k$ and $k'$ shows a conical shape.	7
1.3	Plot of the number of publications per year on carbon materials in the last 50 years.	11
2.1	The honeycomb lattice of graphene. The primitive unit cell is the dashed lines regions with a basis of two atoms A and B, $\theta$ between $\vec{a}_1$ and $\vec{a}_2$ is $60^\circ$ .	16
2.2	The 2D $k$ -space of graphene. The shaded area shows the first Brillouin zone with the high symmetry points $\Gamma$ , M, and $k$ . $k$ and $k'$ are Dirac points	17
2.3.1	The two dimensional direct lattice of a carbon nanotube with the primitive lattice vectors $\vec{a}_1$ and $\vec{a}_2$ , chiral vector $\vec{C}_h$ , and translational vector $\vec{T}$	19
2.3.2	Single-wall carbon nanotubes with different geometries (m, n) types. (a) an "armchair" (n, n) nanotubes, (b) a "zigzag" (m, 0) nanotubes, and (c) a "chiral" (m, n) nanotube $m \neq n$	21
2.4	A schematic plot for nanotubes with both types: (a) a zigzag nanotube where $k_y$ is constrained according to the equation $k_y  \vec{C}_h  = 2\pi\nu$ . (b) An armchair nanotube where $k_x$ is constrained by the condition $k_x  \vec{C}_h  = 2\pi\nu$	25
2.5	The special points of graphene first Brillouin zone	31
2.6	The focus on the Dirac points in the dispersion relation of the graphene which show a conical shape	34
3.1.1	The scaled energy as function of $k_x$ and $k_y$ of graphene.	44
3.1.2	The energy (in eV) of the graphene for	45

	arbitrary $k_y$ values and particular restricted $k_x$ values ( $k_x a = 0$ ).	
3.2.1	The eigen energies of a zigzag nanotube against the wave vector $k_x$ for $m$ and different $\nu$ values showing metallic character (zero gap).	47
3.2.2	The eigen energies of a zigzag nanotube versus the wave vector $k_x$ for $m$ and different $\nu$ values showing semiconducting character (finite energy gap).	48
3.3	The bandgap in (eV) of semiconducting Zigzag CNTs for different ranges of the diameter.	50
3.4.1	The linear behavior of the DOS of graphene for different $m$ and $d$ values.	52
3.4.2	DOS for a metallic zigzag nanotube against the energy $E$ .	54
3.4.3	DOS for a semiconducting zigzag nanotube against the energy $E$ .	55

## List of Abbreviations

$D_{ZCNT}(E)$	Density of State of Zigzag Carbon Nanotube.
$D_g(E)$	Density of States of Graphene.
$E_F$	Fermi Energy.
$E_g$	Energy Gap.
$a_0 \equiv a_{c-c}$	Carbon-Carbon Bond Length.
$g_d$	Greatest Common Divisor.
$m^*$	Effective Mass
$m^2 g^{-1}$	Meter Square per Gram
$v_f$	Fermi Velocity
$\psi_g(\vec{r})$	Graphene Wave Function.
$\psi_{nt}(\vec{r})$	Nanotube Wave function.
0D	Zero Dimensions.
1D	One Dimension.
2D	Two Dimensions.
3D	Three Dimensions.
c	Speed of Light.
CNTs	Carbon Nanotubes.
DOS	Density of States.
E-K	Energy Dispersion Relation.
Eq.	Equation
eV	Electron Volt.
Fig.	Figure
$\hbar$	Reduced Plank Constant.
m/s	Meter per Second
MWCNT	Multi Wall Carbon Nanotube.
nm	Nanometer.
QDS	Quantum Dots.
QSE	Quantum Size Effect.
QWWS	Quantum Well Wires.
SWCNTs	Single Wall Carbon Nanotubes.
T.B	Tight Binding
TPa	Tera Pascal.
$a$	Lattice Constant.
$cm^2 v^{-1} s^{-1}$	Centimeter Square per Volt Second
$wm^{-1} K^{-1}$	Watts per meter Kelvin
ZCNT	Zigzag Carbon Nanotube
$\alpha$	Fine Structure Constant

**The Electronic Band Structure of Graphene and Carbon Nanotubes****By****Asmahan Anan Sulaiman Tiryaki****Supervisor****Prof. Mohammad ELSAID****Co-Supervisor****Dr. Musa ELHASAN****Abstract**

The density of states expressions for graphene and Zigzag carbon nanotubes for different geometries had been rederived using the dispersion relation obtained by the well-known tight-binding method. In addition, our numerical results for the density of states of graphene and zigzag carbon nanotubes had been produced and the results support both the conducting and the semiconducting behavior of the nanotubes. Also we had been used the derived expression for the energy gap of the semiconducting zigzag carbon nanotubes to compute it numerically. Furthermore, we had studied the relativistic Dirac Hamiltonian behavior of the particle in graphene material near the Dirac points and the particle is found to behave as a massless particle. We also compared our numerical results against the very recently experimental and theoretical reported ones.

# **Chapter One**

## **Introduction**

## Introduction

Nanoscience is the study of materials whose physical size is on the nanometer scale in the range of (1-100nm). The new properties of these nanosystems are mainly due to two important factors: (i) surface to volume ratio and (ii) quantum size effect (QSE). The surface to volume ratio for a cube is:  $\frac{S}{V} = \frac{6L^2}{L^3} = \frac{6}{L}$ . As the length L becomes small,  $\frac{S}{V}$  becomes large and so the number of surface atoms will be large. Thus, the smaller the system, the more its surfaces must affect its actual properties. Consequently, the chemical activity of the material can be improved as the material is reduced in size at the nanoscale. The properties of nanosystems are significantly affected by minor changes in size, shape and type of materials. In summary, at the nanoscale, properties become strongly size –dependent. The new developments in fabrication methods, like top-down and bottom-up approaches enable us to confine the carriers in various dimensions: bulk (3D), quantum wells (2D), quantum well wires (QWWS) (1D) and quantum dots (QDS) (0D). The quantum size effect greatly changes the dependence of the density of states  $D(E)$  on the energy E for these systems as follows:

$$D(E) \sim \sqrt{E} \quad \text{in 3D} \quad (1.1)$$

$$D(E) \sim \text{constant} \quad \text{in 2D} \quad (1.2)$$

$$D(E) \sim \frac{1}{\sqrt{E}} \quad \text{in 1D} \quad (1.3)$$

$$D(E) \sim \sum_{\nu} \delta(E - E_{\nu}) \quad \text{in 0D} \quad (1.4)$$

The dependence of the density of states on the dimensionality will lead to a considerable change in the properties of the nanosystems as we mentioned earlier.

One of the nanomaterials that had been discovered very recently, in (2004), and shows very attractive novel properties is the graphene. Graphene becomes the object of intense theoretical and experimental studies. It is a one atom thick sheet of carbon atoms arranged laterally in a honey-comb lattice. The lattice has two carbon atoms A and B, per unit cell, and is invariant under  $120^\circ$  rotations around any lattice site.

(A. K. Geim, 2007) [1].

A few years ago research group at the University of Manchester led by Geim succeeded in isolating and studying graphene. The original method of graphene production is based on micromechanical cleavage of graphite surface the so called (scotch –tape –method) of graphite, in this method a piece of graphite-the material from which the pencils are made-is gently rubbed on a piece of ordinary scotch tape. This produces carbon debris. The scotch tape with the debris is then pressed against a slab of oxidized silicon of 300 nm width. As a consequence the debris moves to the oxidized silicon. Using an optical microscope one can identify small crystalline of graphene on top of the oxidized silicon.

(N. M. Peres, 2009) [2].

Each carbon atom with an atomic number of six has an electronic configuration of  $1S^2 2S^2 2P^2$  (Mandar. M. Deshmukh and Vibhor Singh, 2011) [3].

The  $1S$  electrons are essentially inert and do not contribute to the chemical bond (N. M. Peres, 2009) [2]. In graphene, the  $2S$ ,  $2P_x$  and  $2P_y$  orbital of carbon atom combine (or hybridize) to form three new planners orbital called  $SP^2$  (which will originate the sigma  $\sigma$  bonds). The mechanical properties of graphene are determined by the rigidity of the bond. The remained orbital  $P_z$  (one electron) is perpendicular to the plane formed by the carbon atoms. The  $2P_z$  orbital from different atoms combine to form pi bonds  $\pi$  (valence) and  $\pi^*$ (conduction) bands. Each  $P_z$  orbital contribute with one electron, therefore graphene is a system with one electron per lattice site. This is called a half-filled system (H. S. Philip Wong and Deji Akinwande, 2011) [4]. The pi-orbitals are responsible for the unusual electronic properties of graphene (N. M. Peres, 2009) [2]. A hybridization of  $SP^2$  character leads to hexagonal symmetry as seen in graphite, graphene and carbon nanotubes (CNTs) (M. M. Deshmukh and V. Singh, 2011) [3].

It should be noted that graphene can be considered the raw material for other existing form of pure carbon. For example, wrapping graphene into a sphere produces buckyballs (fullerenes), folding into a cylinder produces nanotubes, and stacking several sheets of graphene leads to graphite (H. S. Philip Wong and Deji Akinwande, 2011) [4] as shown in Fig. 1.1.

The important physics of graphene takes place close to the Dirac points; the equation describing the Low-energy physics in graphene is not the Schrodinger equation as in condensed matter physics, but the massless Dirac equation in (2D); so one moves from electrons interacting with a periodic potential to free massless Dirac particles moving with  $v_f = 10^6 m/s$ , the Fermi velocity (N. M. Peres, 2009) [2].

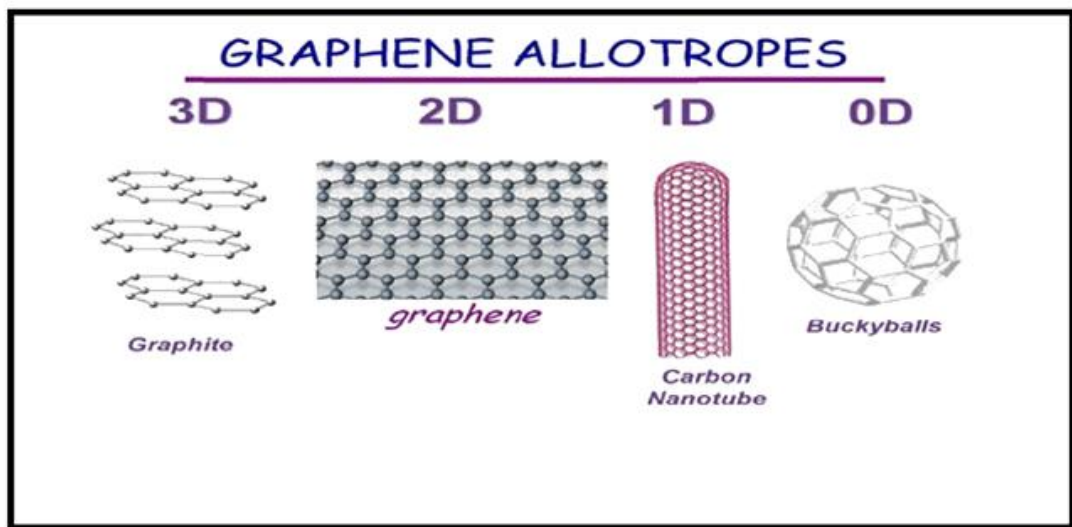


**Fig. 1.1:** Graphene as the source of three different nanomaterial systems: 3D, 2D, 1D and 0D (Leonid Levitov, 2008) [5].

The electronic properties of the two dimensional nanosystem “graphene” close to the Dirac points has a linear dispersion at low energies makes the electrons and holes in graphene mimic relativistic particles that are described by the Dirac relativistic equation for particles with spin 1/2, and they are usually referred to as Dirac fermions. Their dispersion relation  $E = \pm \hbar v_f |\vec{k}| = \pm \hbar v_f \sqrt{k_x^2 + k_y^2}$ , is analogous to that of photons,  $E = \pm \hbar c |\vec{k}|$ , but with the velocity of light  $c$  replaced by  $v_f$ , the Fermi velocity. Thus electrons and holes in graphene have zero effective

mass and velocity which is about 300 times slower than the speed of light. The linear dispersion relationship also means that quasi-particles in graphene display properties different to those observed in conventional (3D) materials, which have parabolic dispersion  $E = \hbar^2 k^2 / 2m^*$  (P. Avouris et al., 2007) [6]; Graphene is an exception: its charge carriers mimic relativistic particles and are easier to describe starting with the Dirac equation rather than the Schrodinger equation (A. K. Geim and K. S. Novoselov, 2007) [7].

In neutral graphene sheet, the valance and conduction bands meet at the Fermi energy so that graphene is a semi-metal or zero-gap semiconductor. The bands form conical valleys that touch at two of the high symmetry points, labeled as  $k$  and  $k'$  in the Brillouin Zone as shown in Fig. 1.2. Near these points the energy varies linearly with the magnitude of momentum. The four other Brillouin Zone corners are related to  $k$  and  $k'$  by reciprocal lattice vectors (N. M. Peres, 2009) [2].

Graphene has a number of fascinating properties. For example, the material is chemically stable, has high thermal conductivity, and has ballistic transport over submicron scale (N. M. Peres, 2009) [2]. An effect of Dirac electrons in graphene is the transparency of material to light. It is found that the transmissivity  $T$  (percentage of light passing through the material) of graphene is given by:  $T = (1 - \pi\alpha) \approx 98\%$ , where  $\alpha$  is fine structure constant (N. M. Peres, 2009) [2].

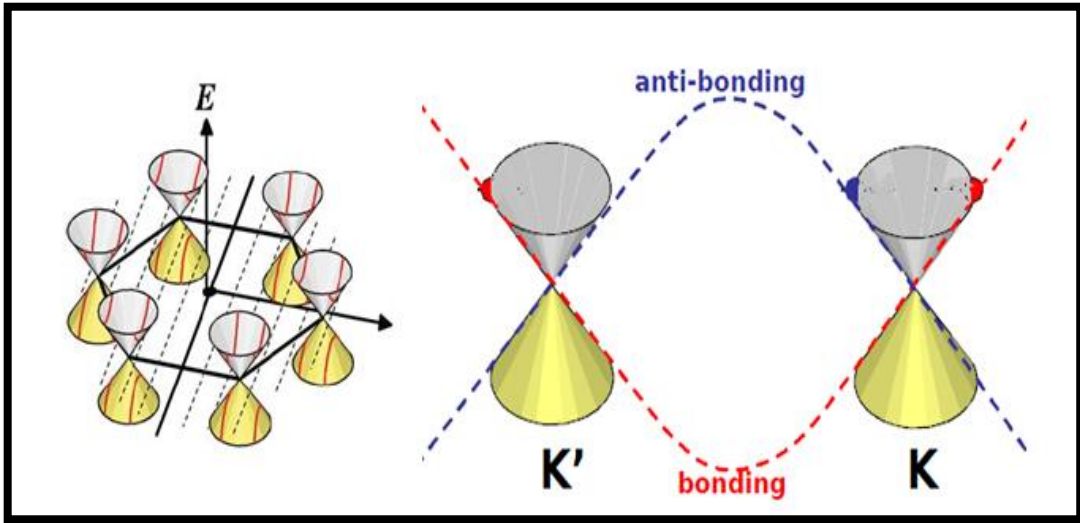


**Fig. 1.2:** The band structure of graphene near the Dirac point's  $k$  and  $k'$  shows a conical shape (Michael Fuhrer and Ellen Williams, 2008) [8].

Graphene is the thinnest material in the universe and the strongest one, have the smallest effective mass (it is zero) and can travel micrometer a long distance without scattering at room temperature (A. K. Geim, 2009) [9]. It has a large theoretical specific surface area ( $2630 \text{ m}^2 \text{ g}^{-1}$ ), high intrinsic mobility ( $200\,000 \text{ cm}^2 \text{ v}^{-1} \text{ s}^{-1}$ ), high Young modulus ( $\sim 1.0 \text{ TPa}$ ) and thermal conductivity ( $\sim 5000 \text{ w m}^{-1} \text{ K}^{-1}$ ) (Y. Zhu et al., 2010) [10].

The structures of carbon nanotubes (which are made by rolling up graphene) are specified by a pair of integers  $(m,n)$  defining the chiral  $\vec{C}_h = m \vec{a}_1 + n \vec{a}_2$  vector, that describes the circumference of the nanotube ( $|\vec{C}_h| = \pi d_{CNT}$ ), where  $\vec{a}_1$  and  $\vec{a}_2$  are unit vectors of the graphene honeycomb lattice and  $d_{CNT}$  is the diameter of the nanotube. The periodic boundary conditions around the circumference of a nanotube require that the component of the momentum along the circumference  $\vec{k}_\perp$  is quantized:  $\vec{C}_h \cdot \vec{k}_\perp = 2\pi \nu$ , where  $\nu$  is a non-zero integer (Ji-Yong Park, 2009) [11]. On the other hand, electron motion along the length of the tube

is free and  $\vec{k}_{\parallel}$  is continuous. The quantization on  $\vec{k}_{\perp}$  leads to the formation of the metallic and semiconducting nanotube materials as we will see.

## 1.1 Research Objectives:

The objectives of this thesis can be summarized as follows:

- 1) In this work the well-known tight binding (T.B) method had been used to derive a closed form dispersion relation (E-K) for the graphene and zigzag carbon nanotube (ZCNT) materials.
- 2) The obtained energy expression had been used to derive the density of states (DOS), energy gap and to calculate the band structures for Zigzag and Chiral CNTs, in order to understand the metallic and semiconducting behavior of the CNT materials. In addition, the electron Dirac Hamiltonian for the CNT near Dirac points  $k$  and  $k'$  also had been derived.
- 3) The obtained expressions had been numerically displayed.

## 1.2 Literatures Review:

Many authors had used the tight-binding method to study the band structure of the graphene materials. For example, the authors in different works (S. Datta, 2005 [12], R. Saito et al., 1998 [13], H. S. Philip Wong et al., 2011 [4] and Ji-Yong Park, 2009 [11]) had used the tight-binding approximation method to investigate the energy levels of a sheet of graphene by finding the energies of the tight-binding Hamiltonian. Gracium et al (S. Russo M. F. Gracium et al., 2009) [14] had also

calculated the energy bands of graphene materials made from monolayer and few layers.

The theory of graphene was first explored in 1947 as a starting point for understanding the electronic properties of more complex, 3D graphite. The emergent massless Dirac equation was first pointed out by David P. De Vincenzo and Eugene J. Mele (en. Wikipedia. org) [15].

Graphene is a relatively new material. In the 1930s, physicists believed that a two dimensional plane was not stable enough to exist independently. (Ron Beech, 2011) [16].

CNTs were first discovered by Iijima in 1991 (S. Iijima, 1991) [17] when he was studying the synthesis of fullerenes. CNTs that Iijima observed were so called multi-walled carbon nanotubes (MWCNTs).

Two years later, single-walled carbon nanotubes (SWCNTs), these thin, hollow cylinders of carbon were discovered in 1993 by groups led by Sumio Iijima at the NEC Fundamental Research Laboratory in Tsukuba, Japan, and by Donald Bethune at IBM's Almaden Research Centre in California. The mass production of CNTs was done in 1995 by Rick Smalley's group at Rice University in Texas (P. L. Mc Euen, 2000) [18].

Spires and Brown had measured the carbon bond length of 0.142 nm in 1996 (T. Spires and R. Brown, 1996) [19].

A single -wall CNTs is a graphene sheet rolled into a cylindrical shape with a diameter of about (0.7-2.0) nm but a multi-wall carbon nanotubes comprises a number of graphene sheets rolled concentrically with an inner diameter of about 5 nm (Edris Faizabadi, 2011) [20].

CNTs according to their structures are classified to three types: armchair, zigzag, and chiral. Armchair and zigzag nanotubes are defined by a carbon nanotube whose mirror image has an identical structure to the original one. On the contrary, chiral nanotubes mirror image cannot be superposed on the original one (Edris Faizabadi, 2011) [20].

For a general  $(m, 0)$  zigzag nanotubes, if  $m$  is a multiple of three, the nanotube becomes metallic as the energy gap at  $k = 0$  becomes zero; however, if  $m$  is not a multiple of three, the nanotube becomes semiconducting because an energy gap which is proportional to nanotube diameter opens at  $k = 0$  (Edris Faizabadi, 2011) [20].

Variety of probes predicts that armchair (SWNTs) is always metallic and all other tubes (zigzag and chiral), depend on whether they satisfy  $(m - n = 3\nu)$  or not (where  $\nu$  is an integer), are metallic or semi-metallic (Edris Faizabadi, 2011) [20].

Andre Geim and Konstantin Novoselov came up with a method after years of effort to isolate monolayer graphene Flakes. They developed scotch-tape method in 2004 and they were awarded the Nobel Prize for their discovery in 2010 (M. M. Deshmukh and V. Singh, 2011) [3].

$sp^2$  Carbon nanomaterial, notably (0D) Fullerenes, (1D) (CNTs), and (2D) graphene have gained significant interest from various fields since their discovery in 1985, 1991 and 2004, respectively (Y. Zhu et al., 2010) [10].

Devices made from metallic (SWCNTs) were first measured in 1997. While, devices made from semiconducting (SWCNTs) were first reported by Tans et al. in 1998 (Paul L. McEuen and Ji-Yong Park, 2004) [21].

The recent developments in the study of graphene were fueled by a 2004 paper by Novoselov et al. that has made a large impact on researchers working in the field of carbon nanotubes, as shown by the recent surge in publications on carbon nanostructures as shown in Fig. 1.3 (M. S. Dresselhaus, 2012) [22].

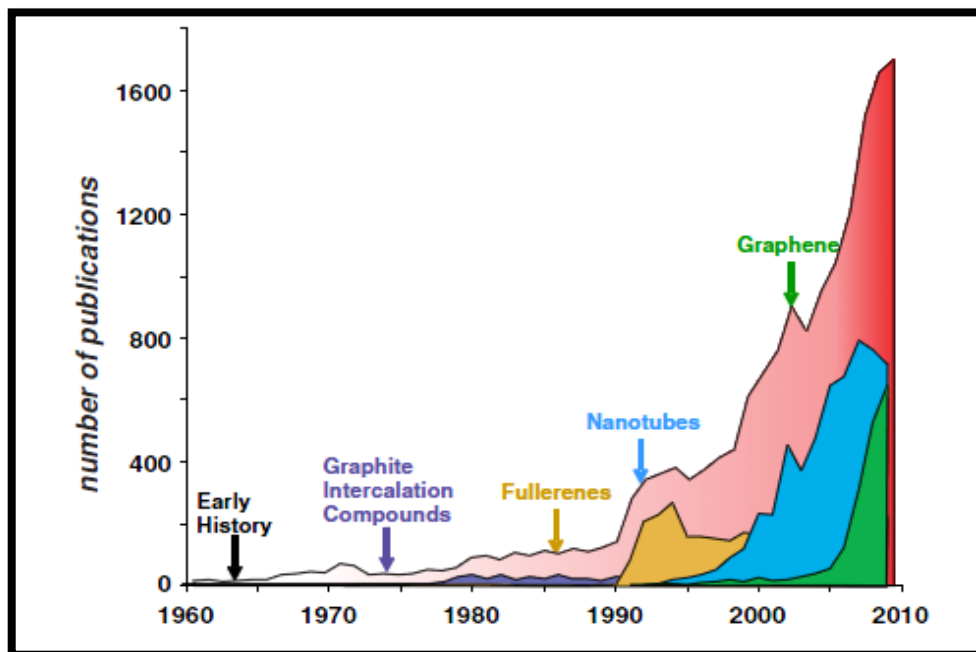


**Fig. 1.3:** plot of the number of publications per year on carbon materials in the last 50 years (M. S. Dresselhaus, 2012) [22].

### 1.3 Method of Calculations:

In this work, the well known tight binding approximation, as an efficient method, had been used to derive a closed form expression for the dispersion relation  $E(k_x, k_y)$  of the graphene sheet in terms of the momentum components,  $k_x$  and  $k_y$ , the lattice constant  $a$ , and the transfer integral / or the strength of the nearest neighbor hopping,  $\gamma_0 = 2.9 \text{ eV}$ . The obtained energy expression had been used to calculate the electronic band structure of graphene and zigzag nanotube which corresponds to the case ( $n=0$ ) or  $\vec{C}_h = (m, 0)$ . All other chiral vectors  $\vec{C}_h = (m, n)$ ,  $0 < m < n$  correspond to Chiral nanotubes had been also studied.

Our numerical results for the electronic band structure of the CNTs had shown the behavior of the material as a metal and as a semiconductor. This very interesting metallic and semiconducting behavior of carbon nanotubes had also been reported both theoretically and experimentally (Ji- Yong Park, 2009) [11] and (S. Datta, 2005) [12]. In addition, we had been derived expressions for the density of states for the graphene and carbon nanotube materials.

The organization of the thesis is given as follows. In chapter 1 we have presented an introduction to the nanomaterials: graphene and carbon nanotubes. The theory and the tight binding calculation method for the graphene and carbon nanotubes are discussed in chapter 2. We have given

the numerical results and discussion in chapter 3. Finally, chapter 4 is devoted for the conclusions.

# **Chapter Two**

## **Theory**

## Theory

The objective of this chapter is to describe the basic theoretical background for the physical and electronic structure of graphene and carbon nanotubes.

### 2.1 Direct Lattice Structure of Graphene:

Graphene is a two dimensional one atom thick planar sheet of  $SP^2$  bonded carbon atoms densely packed in a honeycomb structure (Rene Petersen, 2009) [23] as shown in Fig. 2.1.

The basis vector that generates the graphene lattice is:

$$\vec{a}_1 = a \cos 30^\circ \hat{x} + a \sin 30^\circ \hat{y} = \left(\frac{\sqrt{3}a}{2}, \frac{a}{2}\right) \quad (2.1)$$

$$\vec{a}_2 = a \cos 30^\circ \hat{x} - a \sin 30^\circ \hat{y} = \left(\frac{\sqrt{3}a}{2}, \frac{-a}{2}\right) \quad (2.2)$$

with  $|\vec{a}_1|=|\vec{a}_2|=a = \sqrt{3}a_{c-c}$ ,  $\vec{a}_1 \cdot \vec{a}_1 = \vec{a}_2 \cdot \vec{a}_2 = a^2$ ,  $\vec{a}_1 \cdot \vec{a}_2 = a^2/2$ , where  $a_{c-c} \approx 0.142$  nm is the carbon-carbon bond length, A and B are the two atoms in the unit cell of graphene and these contribute a total of two  $\pi$  electrons per unit cell to the electronic properties of graphene (H. S. Philip Wong and Deji Akinwande, 2011) [4].

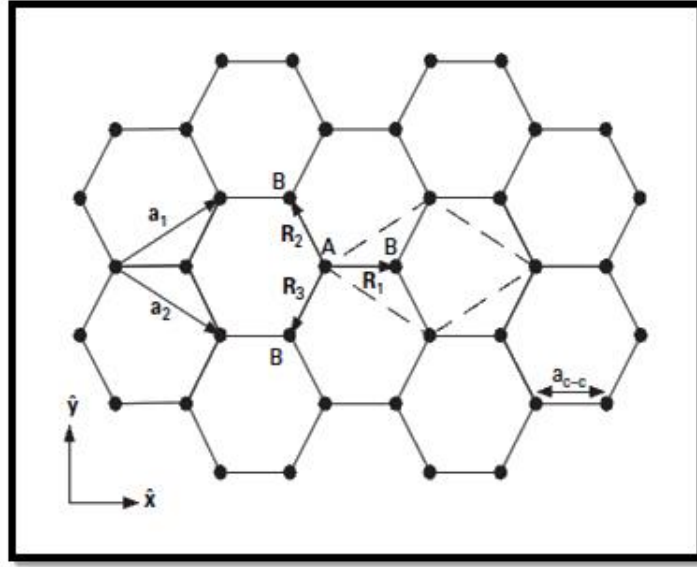


**Fig. 2.1:** The honeycomb lattice of graphene. The primitive unit cell is the dashed lines region with a basis of two atoms A and B, the angle  $\theta$  between  $\vec{a}_1$  and  $\vec{a}_2$  is  $60^\circ$  (H. S. Philip Wong and Deji Akinwande, 2011) [4].

The primitive unit cell can be considered as equilateral parallelogram with side  $a = \sqrt{3}a_{c-c} = 0.246$  nm where  $a$  is the lattice constant of graphene (Davood Fathi, 2011) [24].

Each carbon atom is bonded to its three nearest neighbors and the vectors describing the separation between type A atom and the nearest neighbor type B atoms (H. S. Philip Wong and Deji Akinwande, 2011) [4] are:

$$\vec{R}_1 = \frac{a}{\sqrt{3}} \hat{x} = \left(\frac{a}{\sqrt{3}}, 0\right) \quad (2.3)$$

$$\vec{R}_2 = -\vec{a}_2 + \vec{R}_1 = -\frac{a}{2\sqrt{3}} \hat{x} - \frac{a}{2} \hat{y} = \left(-\frac{a}{2\sqrt{3}}, -\frac{a}{2}\right) \quad (2.4)$$

$$\vec{R}_3 = -\vec{a}_1 + \vec{R}_1 = -\frac{a}{2\sqrt{3}} \hat{x} + \frac{a}{2} \hat{y} = \left(-\frac{a}{2\sqrt{3}}, \frac{a}{2}\right) \quad (2.5)$$

with  $|\vec{R}_1| = |\vec{R}_2| = |\vec{R}_3| = a_{c-c} = 0.142$  nm.

## 2.2 The Reciprocal Lattice of Graphene:

The reciprocal lattice of graphene shown in Fig. 2.2 is also a hexagonal lattice but rotated  $90^\circ$  with respect to the direct lattice. The reciprocal lattice vectors are:

$$\vec{b}_1 = 2\pi \frac{(\vec{a}_2 \times \vec{a}_3)}{\vec{a}_1 \cdot \vec{a}_2 \times \vec{a}_3} = \left( \frac{2\pi}{a\sqrt{3}}, \frac{2\pi}{a} \right) = \frac{2\pi}{a\sqrt{3}} \hat{k}_x + \frac{2\pi}{a} \hat{k}_y \quad (2.6)$$

$$\vec{b}_2 = 2\pi \frac{(\vec{a}_3 \times \vec{a}_1)}{\vec{a}_1 \cdot \vec{a}_2 \times \vec{a}_3} = \left( \frac{2\pi}{a\sqrt{3}}, -\frac{2\pi}{a} \right) = \frac{2\pi}{a\sqrt{3}} \hat{k}_x - \frac{2\pi}{a} \hat{k}_y \quad (2.7)$$

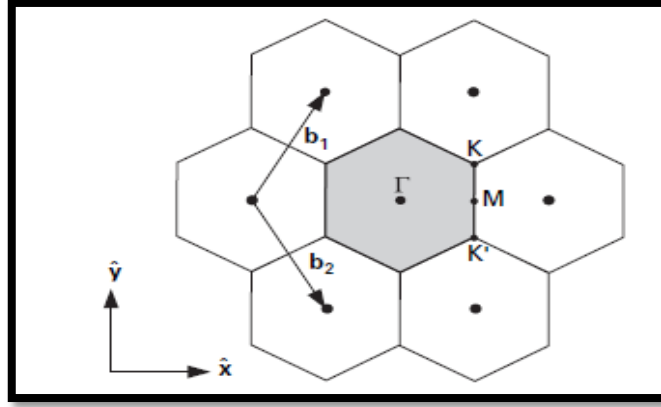


**Fig. 2.2:** The 2D  $k$ -space of graphene. The shaded area shows the first Brillouin zone with the high symmetry points  $\Gamma$ ,  $M$ ,  $k$  and  $k'$ .  $k$  and  $k'$  are Dirac points and they are equivalent (H. S. Philip Wong and Deji Akinwande, 2011) [4].

$|\vec{b}_1| = |\vec{b}_2| = 4\pi/(a\sqrt{3})$ . There are three key locations of high symmetry in the Brillouin zone. These locations are the  $\Gamma$ -point, the  $M$ -point, and the  $k$ -point. The  $\Gamma$ -point is at the center of the Brillouin zone,  $\vec{\Gamma M} = (2\pi/a\sqrt{3}, 0)$  and  $\vec{\Gamma k} = (2\pi/a\sqrt{3}, 2\pi/3a)$  (H. S. Philip Wong and Deji Akinwande, 2011) [4].

### **2.3 Carbon Nanotubes (CNTs):**

A single-wall carbon nanotube (SWCNT) can be observed as a single sheet of graphite rolled up into a cylinder with diameter varying from 0.6 to about 3nm (Davood Fathi, 2011) [24]. CNTs were discovered in 1991 by the Japanese Sumio Iijima when he was studying the synthesis of fullerenes (Wen-Shing Jhang, 2006) [25].

If just one layer of graphite is rolled-up into a cylinder, the single cylinder is called a single walled carbon nanotube (SWCNT). If  $n$  layers are rolled around each other, the result is  $n$  concentric tubes; the concentric tubes are called a multi-walled carbon nanotube (MWCNT). The focus is on (SWCNT) because they are a simpler system. For now, we will restrict our discussion to single-walled nanotubes (Luke Anthony Kaiser Donev, 2009) [26].

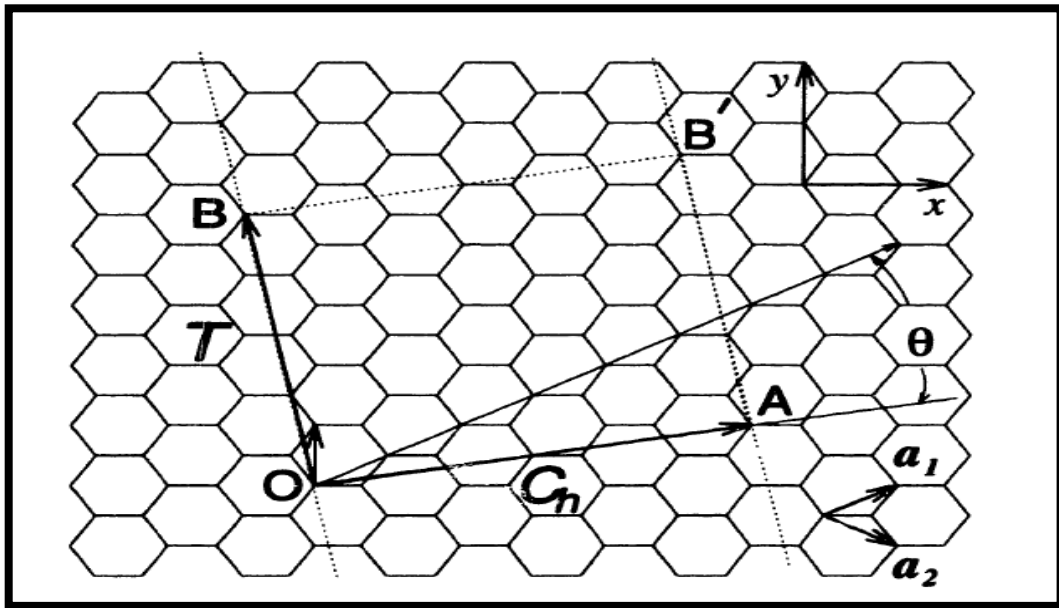
Carbon nanotubes are considered as one dimensional nanomaterial owing to their very small diameter that confines electrons to move along their length, all single-wall CNTs are either chiral (not superimpose on its mirror image) or achiral (superimpose on their own mirror image). Achiral CNTs are classified as armchair CNTs or zigzag CNTs (H. S. Philip Wong and Deji Akinwande, 2011) [4].

Fig. 2.3.1 represents the two dimensional hexagonal plane that makes up a graphite sheet, where the carbon atoms lie at the corners of each hexagon. In the figure, if point O is connected to point A, and point B is connected to

point  $B'$ , then one will observe that the sheet will be rolled into a cylindrical structure; as a result a nanotube can be constructed (Rashid Nizam et al., 2011) [27].

$\overrightarrow{OA}$  and  $\overrightarrow{OB}$  define the chiral vector  $\overrightarrow{C}_h$  and the translational vector  $\overrightarrow{T}$  of the nanotube respectively. The rectangle  $OABB'$  defines the unit cell for the nanotube (Sandra D. M. Brown, 2000) [28].

Fig. 2.3.1 shows the honeycomb lattice of graphene and the primitive lattice vectors  $\overrightarrow{a}_1$  and  $\overrightarrow{a}_2$ .



**Fig. 2.3.1:** The two dimensional direct lattice of a carbon nanotube with the primitive lattice vectors  $\overrightarrow{a}_1$  and  $\overrightarrow{a}_2$ , chiral vector  $\overrightarrow{c}_h$ , and translational vector  $\overrightarrow{T}$  (Rashid Nizam et al., 2011) [27].

The CNT is characterized by three geometrical parameters, the chiral (circumferential) vector  $\overrightarrow{C}_h$ , the translation vector  $\overrightarrow{T}$ , and the chiral angle  $\theta$  (H. S. Philip Wong and Deji Akinwande, 2011) [4] as shown in Fig. 2.3.1.

The chiral vector is the geometrical parameter that uniquely defines a CNT which is the vector connecting any two primitive lattice points of graphene such that when folded into a nanotube these two points are indistinguishable,  $\vec{C}_h = m\vec{a}_1 + n\vec{a}_2 = (m, n)$  for which the CNT diameter can be obtained by:

$$d = \frac{|\vec{C}_h|}{\pi} = \frac{a\sqrt{n^2+m^2+nm}}{\pi} \quad (2.8)$$

where (m, n are positive integers). A type of CNT can be deduced directly from the values of the chiral vector. In the first case, if  $m = n$ , then the angle  $\theta$  will be  $30^\circ$ ; the carbon bonds form an armchair shaped pattern, so all (n, n) CNTs are armchair nanotubes. In the second case, when  $\vec{C}_h$  is purely along the direction of  $\vec{a}_1$ , ( $\vec{C}_h = (m, 0)$ ),  $\theta = 0^\circ$  and the bonds along the chiral vector form a zigzag pattern the result is zigzag nanotubes. In the third case,  $0^\circ \leq \theta \leq 30^\circ$  and the tubes are known as chiral nanotubes (Rashid Nizam et al., 2011) [27] as shown in Fig. 2.3.2. The chiral angle is the angle between the chiral vector and primitive lattice vector  $\vec{a}_1$  where:

$$\cos \theta = \frac{2m+n}{2\sqrt{n^2+m^2+nm}} \quad (2.9)$$

The translation vector defines the periodicity of the lattice along the tubular axis. Geometrically,  $\vec{T}$  is the smallest graphene vector perpendicular to  $\vec{C}_h$ .

Let  $\vec{T} = C\vec{a}_1 + D\vec{a}_2$ , where C and D are integers. The translation vector can be calculated from the orthogonality condition  $\vec{C}_h \cdot \vec{T} = 0$ . So,

$$\vec{T} = \left( \frac{2n+m}{g_d} \vec{a}_1, \frac{-2m+n}{g_d} \vec{a}_2 \right) \quad (2.10)$$

where  $g_d$  is the greatest common divisor of  $(2n+m)$  and  $(2m+n)$ . The length of the cylinder is:

$$|\vec{T}| = \frac{\sqrt{3}}{g_d} |\vec{C}_h| \quad (2.11)$$

where  $|\vec{C}_h| = a\sqrt{n^2 + m^2 + nm}$ . Some results that are useful to compute is the surface area of CNT unit cell, the number of hexagons per unit cell, and the number of carbon atoms per unit cell. The surface area of CNT primitive cell is the area of the rectangle defined by  $\vec{C}_h$  and  $\vec{T}$  vectors as  $|\vec{C}_h \times \vec{T}|$ .

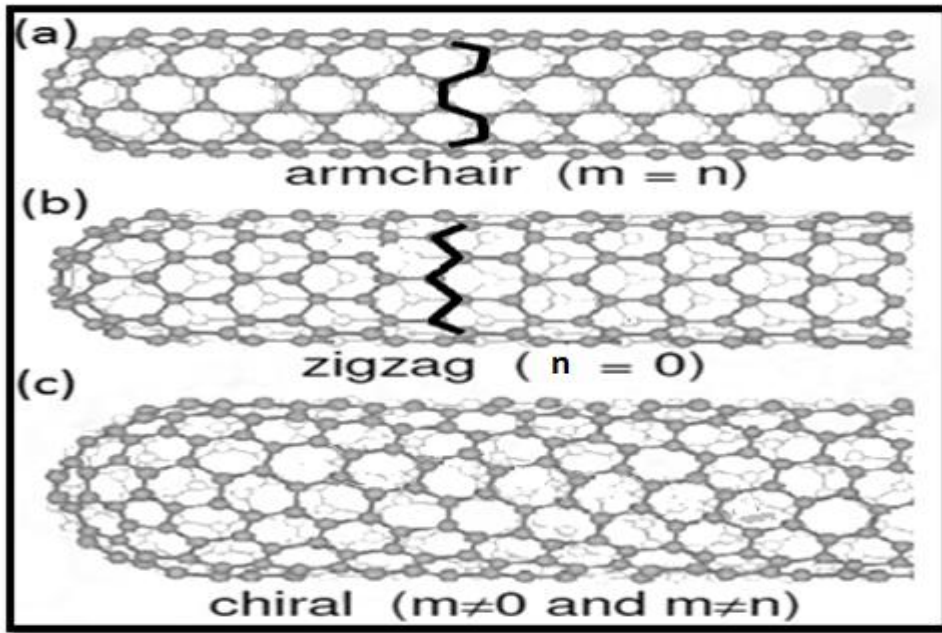


**Fig. 2.3.2:** single-wall carbon nanotubes with different geometries  $(m, n)$  types. (a) an “armchair”  $(n, n)$  nanotubes, (b) a “zigzag”  $(m, 0)$  nanotubes, and (c) a “chiral”  $(m, n)$  nanotube  $m \neq n$  (R. Bruce Weisman, 2010) [29].

The number of hexagons per unit cell  $N$  is the surface area divided by the area of one hexagon:

$$N = \frac{|\vec{C}_h \times \vec{T}|}{|\vec{a}_1 \times \vec{a}_2|} = 2 \frac{|\vec{C}_h|^2}{a^2 g_d} \quad (2.12)$$

Since there are two carbon atoms per hexagon, there are a total of  $2N$  carbon atoms in each CNT unit cell.

## 2.4 Graphene Rolling-Up:

As we said that CNTs can be obtained by rolling up a sheet of graphite into a cylinder which results in additional quantization to the graphene band structure, such that the phase of an electron going around the circumference of the nanotube must be an integer multiple of  $2\pi$  as follows (Luke Anthony Kaiser Donev, 2009) [26]:

The periodic boundary condition for a nanotube wave function  $\psi_{nt}$  is

$$\psi_{nt}(\vec{r}) = \psi_{nt}(\vec{r} + \vec{C}_h) \quad (2.13)$$

Bloch theorem for the nanotube wave function is

$$\psi_{nt}(\vec{r} + \vec{C}_h) = e^{i\vec{k} \cdot \vec{C}_h} \psi_{nt}(\vec{r}) \quad (2.14)$$

Combining (2.13) and (2.14) we get:

$$e^{i\vec{k} \cdot \vec{C}_h} = 1 \rightarrow \vec{k} \cdot \vec{C}_h = 2\pi \nu$$

where  $\nu$  is a non-zero integer.

Nanotube states are the same as the set of graphene state in directions in reciprocal space that satisfy the condition (Ana Dergan, 2010) [30]:

$$\vec{k} \cdot \vec{C}_h = 2\pi \nu \quad (2.15)$$

This defines a series of parallel lines, each corresponding to different integer value of  $\nu$  (S. Datta, 2005) [12].

Two types of folding are of interest: the first is a fold in the  $\hat{y}$  direction which resulting in the Zig-Zag nanotube since the circumferential edge looks like a ZigZag. Second is a fold in  $\hat{x}$  direction resulting in the armchair nanotube (S. Datta, 2005) [12].

A fold in  $\hat{y}$  direction has the circumferential vector  $\vec{C}_h = 2mb\hat{y}$ , where  $m$  is an integer, and the periodic boundary condition then requires the allowed values of  $k$  to lie parallel to  $k_x$  axis described by:

$$k_y = 2\pi \nu / 2bm \quad (2.16)$$

As shown in Fig. 2.4a, a nanotube will only conduct if one of its subbands passes through the six corners of the Brillouin zone. So the condition of conduction is:

$$\frac{2\pi\nu}{2mb} = \frac{2\pi}{3b} \rightarrow \frac{\nu}{2m} = \frac{1}{3} \quad (2.17)$$

Therefore, a Zigzag nanotube will be like a conductor if  $m$  is a multiple of three. If the lines of quantized wave vector do not intersect the graphene Fermi points, the CNT is semiconducting with a band gap.

Rolling in the  $\hat{x}$ -direction, create a tube with ( $\vec{C}_h = 2ma\hat{x}$ ), where  $m$  is an integer. This will result in real periodic boundary conditions because each

point on graphene will coincide with a similar one after being rolled-up. The periodic boundary conditions along the circumference result in:

$$k_x = 2\pi \nu / 2ma \quad (2.18)$$

Here  $k_x$ 's are series lines parallel to  $k_y$  as shown in the Fig. 2.4b.

In general, it is possible to roll-up along any circumferential vector of the form

$(\vec{C}_h = m\vec{a}_1 + n\vec{a}_2)$  , and  $m-n$  must be a multiple of three in order for metallic properties to exist. By substituting the value of  $\vec{a}_1$  and  $\vec{a}_2$  we get:

$$\vec{C}_h = (m + n) \left( \frac{\sqrt{3}}{2} a \hat{i} \right) + (m - n) \left( \frac{a}{2} \hat{j} \right) \quad (2.19)$$

But the requirement of periodic boundary conditions is  $\vec{k} \cdot \vec{C}_h = 2\pi\nu$  . So,

$$(m + n) \left( \frac{\sqrt{3}}{2} a k_x \right) + (m - n) \frac{a}{2} k_y = 2\pi \nu \quad (2.20)$$

This defines a series of parallel lines, each corresponding to different  $\nu$  .

Whether the resulting subband dispersion relation will show an energy gap or not depends on whether one of the lines defined by Eq. 2.20 passes through the center of one of the valleys  $(k_x a, k_y b) = (0, \pm \frac{2\pi}{3})$  (S. Datta, 2005) [12].

So, in order for a line to pass through  $k_x a = 0$ , and  $k_y b = \frac{2\pi}{3}$  we must have  $\frac{m-n}{3} = \nu$  this can only happen if  $(m-n)$  is a multiple of three; nanotubes satisfying this condition are metallic.

If the lines do not pass through the center of one of the valleys, nanotubes satisfying this condition are semiconductor (M. P. Anantram et al., 2006) [31].

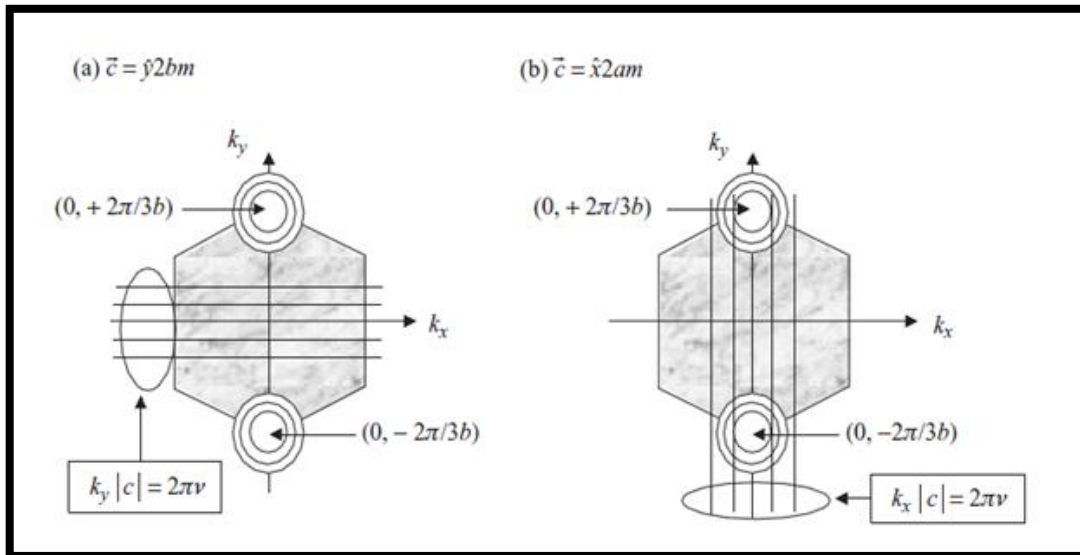


**Fig. 2.4:** A schematic plot for nanotubes with both types: (a) a zigzag nanotube where  $k_y$  is constrained according to the equation  $k_y |\vec{c}_h| = 2\pi\nu$ . (b) An armchair nanotube where  $k_x$  is constrained by the condition  $k_x |\vec{c}_h| = 2\pi\nu$  (S. Datta, 2005) [12].

## 2.5 Electronic Band Structure of Graphene:

The electronic band structure of graphene is very important because (i) it is the starting point for the understanding of graphene's solid state properties and (ii) it is the starting point for the understanding and derivation of the band structure of CNTs (H. S. Philip Wong and Deji Akinwande, 2011) [4].

The origin of the band structure is simply related to the fact that unhybridized  $p_z$  overlap with nearest neighbors to form  $\pi$ -orbitals spread out in energy and give rise to band of states extend over a range of energies (M. M. Deshmukh et al., 2011) [3].

### 2.5.1 Tight Binding Approximation:

The energy band dispersion of graphene can be calculated using a tight-binding model for electrons hopping in the honeycomb lattice. In this approximation we consider only hopping between nearest neighbor atomic sites since the energy contribution from the higher order hopping terms is small (M. F. Craciun et al., 2011) [32].

In this section we will present only the essential mathematical steps which lead to the graphene dispersion relation. We will refer the interested reader to (Ji-Yong Park, 2009) [11] and (H. S. Philip Wong and Deji Akinwande, 2011) [4] references for more details.

In order to derive the band structure of graphene (E- k) relation we solve the Schrödinger equation as follows:

$$\hat{H}\psi = E\psi \quad (2.21)$$

Where  $\hat{H}$  is the Hamiltonian,  $\psi$  is the total wave function, and E is the energy of electrons in the  $\pi$  orbital of graphene (Ji-Yong Park, 2009) [11].

As we said graphene lattice has two carbon atoms, A and B, per unit cell (A. K. Geim, 2007) [1]. So the total wave function  $\psi$  can be written as a linear combination of two Bloch functions  $u_A$  and  $u_B$  as follows:

$$\psi(\vec{k}, \vec{r}) = c_A u_A(\vec{k}, \vec{r}) + c_B u_B(\vec{k}, \vec{r}) \quad (2.22)$$

By substituting Eq. 2.22 in Eq. 2.21, multiplying by the complex conjugate of  $u_A^*$  and  $u_B^*$  and integrating over the entire space, we can write the Schrödinger equation in (2.21) in matrix form as follows:

$$\begin{pmatrix} H_{AA} & H_{AB} \\ H_{BA} & H_{BB} \end{pmatrix} \begin{pmatrix} c_A \\ c_B \end{pmatrix} = E \begin{pmatrix} S_{AA} & S_{AB} \\ S_{BA} & S_{BB} \end{pmatrix} \begin{pmatrix} c_A \\ c_B \end{pmatrix} \quad (2.23)$$

where the matrix elements are defined as follows:

$$H_{ij} = \int_{\Omega} u_i^* \hat{H} u_j dr, \quad S_{ij} = \int_{\Omega} u_i^* u_j dr$$

$H_{ij}$  are the matrix elements of the Hamiltonian or transfer integral,  $S_{ij}$  are the overlap matrix elements between Bloch functions.

Since the atoms A and B in the unit cell of the graphene are identical the matrix elements are taken to be equals such that  $H_{AA} = H_{BB}$ ,  $S_{AA} = S_{BB}$  (H. S. Philip Wong and Deji Akinwande, 2011) [4], and the overlapping between wave functions of different atoms is neglected. i. e.,  $S_{BA} = S_{AB} = 0$ , while  $S_{AA} = S_{BB} = 1$  (Ji-Yong Park, 2009) [11].

To get a non-trivial solution for Eq. 2.23, the determinant of this matrix must vanish, namely:

$$\begin{vmatrix} H_{AA} - E & H_{AB} \\ H_{BA} & H_{BB} - E \end{vmatrix} = 0 \quad (2.24)$$

The solution of this determinant gives us the eigenenergies in terms of the matrix elements:

$$E = H_{AA} \pm |H_{AB}| \quad (2.25)$$

To evaluate the matrix elements which are given in Eq. 2.25 the wave functions  $u_A$  and  $u_B$  are taken as a linear combination of wave functions localized at each atom site:

$$u_{A(B)}(\vec{k}, \vec{r}) = \frac{1}{\sqrt{N}} \sum_{A(B)}^N e^{i\vec{k} \cdot \vec{r}_{A(B)}} X(\vec{r} - \vec{r}_{A(B)}) \quad (2.26)$$

where  $X(\vec{r})$  is the orbital  $2P_Z$  wave function for an isolated carbon atom,  $N$  is the number of the unit cells (Ji-Yong Park, 2009) [11].

We can calculate the diagonal matrix elements ( $H_{AA} = H_{BB}$ ) as follows:

$$H_{AA} = \frac{1}{N} \sum_A \sum_{A^*} e^{i\vec{k} \cdot (\vec{r}_A - \vec{r}_A^*)} \int X^*(\vec{r} - \vec{r}_A) H X(\vec{r} - \vec{r}_A^*) d\tau \quad (2.27)$$

For calculating the matrix elements given by Eq. 2.27 we consider the effect of the three nearest neighbors for each atom A (B):

$$H_{AA} = \int X^*(\vec{r} - \vec{r}_A) H X(\vec{r} - \vec{r}_A^*) d\tau = E_0 = H_{BB} \quad (2.28)$$

$$H_{AB} = \frac{1}{N} \sum_A \sum_{B^*} e^{-i\vec{k} \cdot (\vec{r}_A - \vec{r}_B)} \int X^*(\vec{r} - \vec{r}_A) H X(\vec{r} - \vec{r}_B) d\tau \quad (2.29)$$

$$H_{AB} = \frac{1}{N} \sum_i e^{-i\vec{k} \cdot \vec{R}_i} \int X^*(\vec{r}) H X(\vec{r} - \vec{R}_i) d\tau \quad (2.30)$$

where  $\vec{R}_i$  is a vector connecting atom A to its three nearest neighbor B atoms as shown early in equations 2.3, 2.4, and 2.5.

Eq. 2.30 becomes:

$$H_{AB} = \left( e^{-i\vec{k} \cdot \vec{R}_1} + e^{-i\vec{k} \cdot \vec{R}_2} + e^{-i\vec{k} \cdot \vec{R}_3} \right) \int X^*(\vec{r}) H X(\vec{r} - \vec{R}_1) d\tau \quad (2.31)$$

where  $\int X^*(\vec{r})HX(\vec{r} - \vec{R}_1) d\tau = \gamma_0$  is the transfer integral or the nearest neighbor interaction.

Eq. 2.31 becomes:

$$H_{AB} = \left( e^{-i\vec{k}\cdot\vec{R}_1} + e^{-i\vec{k}\cdot\vec{R}_2} + e^{-i\vec{k}\cdot\vec{R}_3} \right) \gamma_0 \quad (2.32)$$

The matrix element  $H_{AB}$  can be calculating directly by substituting the values of the coordinates of the nearest neighbor vectors  $\vec{R}_i$  ( $i = 1, 2, 3$ ) in Eq. 2.32.

By substituting the obtained matrix element  $H_{AB}$  and it's conjugate  $H_{AB}^*$  in the main energy equation (2.25) to finally obtain an energy expression in a closed form as:

$$E = E_0 \pm |H_{AB}| = E_0 \pm \sqrt{H_{AB}H_{AB}^*}$$

$$E = E_0 \pm \gamma_0 \left( 1 + 4\cos\left(\frac{\sqrt{3}}{2}k_x a\right) \cos\left(\frac{k_y a}{2}\right) + 4\cos^2\left(\frac{k_y a}{2}\right) \right)^{\frac{1}{2}} \quad (2.33)$$

Where  $a = \sqrt{3}a_{c-c} = \sqrt{3}a_0$ .

For the sake of simplicity, we rewrite the dispersion relation in terms of the new parameters  $a = \left(\frac{3a_0}{2}\right)$ , and  $b = \left(\sqrt{3}\frac{a_0}{2}\right)$  as follows:

$$E = E_0 \pm \gamma_0 \left( 1 + 4\cos(k_x a) \cos(k_y b) + 4\cos^2(k_y b) \right)^{\frac{1}{2}} \quad (2.34)$$

The negative and positive signs in Eq. 2.34 refer to the valance and conduction bands respectively (Y. Zhu et al., 2010) [10].

The main feature of the energy dispersion of graphene as we will see in the next chapter is the six  $k$  points at the corners of the Brillouin zone, where the conduction and valance bands meet so that, the band gap is zero only at these points (Ji-Yong Park, 2009) [11].

The six points are also the points at which the Fermi energy cuts two bands and so the solid has six Fermi points (M. M. Deshmukh et al., 2011) [3]. Even more interesting is the form of the valance and conduction bands close to Dirac points, they show a conical shape, with negative (valance) and positive (conduction) energy values (N. M. Peres, 2009) [2] as we are going to show in the coming sections.

If we return to the high symmetry points like  $\Gamma$ , M and  $k$  and substitute their coordinates in Eq. 2.33 we can see that at  $\Gamma$  – point, where  $\vec{k} = 0$ , the two bands are separated by  $6\gamma_0$ . At the M-points, such as  $\vec{k} = \frac{2\pi}{a\sqrt{3}}\hat{k}_x$ , the bands are separated by  $2\gamma_0$ . The vector  $\vec{k}$  of one of the  $k$ -points is  $\vec{\Gamma k} = \frac{1}{3}(2\vec{b}_1 + \vec{b}_2) = \frac{2\pi}{a\sqrt{3}}\hat{k}_x + \frac{2\pi}{3a}\hat{k}_y$  gives  $E_g = 0$ . So at the  $k$  and  $k'$  points, the two bands touch and they called Dirac points (Luke Anthony Kaiser Donev, 2009) [26].

In order to find the Dirac points coordinate we make the determinant of the transfer integral vanishes such that  $|H_{AB}| = 0$  in Eq. 2.34 where the

eigenvalue  $E = \pm|H_{AB}|$  (S. Datta, 2005) [12]. Taking  $E_0 = 0$ , and let  $H_{AB} = h'(\vec{k})$  for simplicity, this lead to the following root equation:

$$|h'(\vec{k})| = \gamma_0 \left( 1 + 4\cos(k_x a)\cos(k_y b) + 4\cos^2(k_y b) \right)^{\frac{1}{2}} = 0.$$

For  $k_x a = 0$ , we have:  $h'(\vec{k}) = \gamma_0(1 + 2\cos(k_y b)) = 0$  and  $k_y b = \pm \frac{2\pi}{3}$ .

But for  $k_x a = \pm\pi$ , we obtain  $k_y b = \pm \frac{\pi}{3}$ .

These six points are special as they provide the states right around the Fermi energy and thus determine the electronic properties. They can be put into two groups; each group has three points as follows:

$$(k_x a, k_y b) = (0, 2\pi/3), (-\pi, -\pi/3), (\pi, -\pi/3)$$

$$(k_x a, k_y b) = (0, -2\pi/3), (-\pi, \pi/3), (\pi, \pi/3)$$

All three within group are equivalent point since they differ by a reciprocal lattice vector as shown in Fig. 2.5. Each group give  $(k_x a, k_y b) = (0, \pm 2\pi/3)$ .

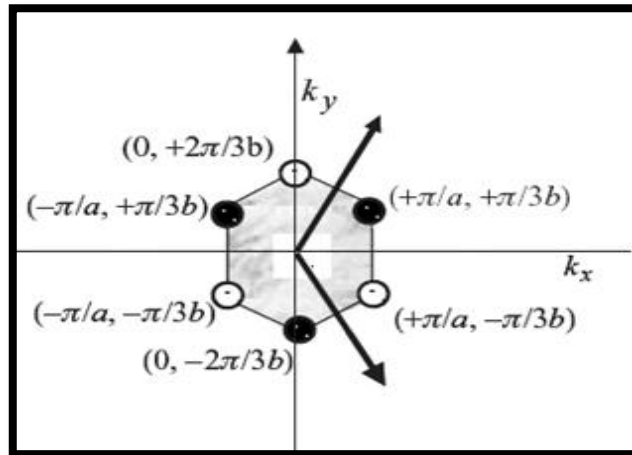


**Fig. 2.5:** The special points of graphene first Brillouin zone (S. Datta, 2005) [12].

## 2.6 The Conical Shape of Graphene Dispersion near the Dirac Points:

Graphene is a half-filled system and therefore, the valance band is completely filled and the conduction band is completely empty (N. M. Peres, 2009) [2].

To understand the electronic properties of graphene we need to investigate the energy and momentum relationship of the graphene near the Fermi energy  $E_f = 0$  (M. M. Deshmukh et al., 2011) [3].

For achieving this goal we substitute the values of the nearest neighbor vectors in Eq. 2.32 to get:

$$h'(\vec{k}) = \gamma_0 \left( e^{-\frac{ik_x a}{\sqrt{3}}} + 2e^{\frac{ik_x a}{2\sqrt{3}}} \cos\left(\frac{k_y a}{2}\right) \right) \quad (2.35)$$

Where  $H_{AB} = h'(\vec{k})$ .

If we multiply Eq. 2.35 by  $e^{\frac{ik_x a}{\sqrt{3}}}$  it can be written it in terms of a and b as follows:

$$h(\vec{k}) = \gamma_0 (1 + 2e^{ik_x a} \cos(k_y b)) \quad (2.36)$$

Where  $h(\vec{k}) = h'(\vec{k}) e^{\frac{ik_x a}{\sqrt{3}}}$ .

In order to find the shape of the dispersion relation of the graphene near the Dirac points we expand  $h(\vec{k})$  from Eq. 2.36 around Dirac points  $(k_x a, k_y b) = (0, \pm \frac{2\pi}{3})$  (S. Datta, 2005) [12]. The Taylor expansion of the  $h(\vec{k})$  can be expressed as:

$$h(\vec{k}) = \left( \frac{dh}{dk_x} \right)_{(k_x a, k_y b) = (0, \pm \frac{2\pi}{3})} k_x + \left( \frac{dh}{dk_y} \right)_{(k_x a, k_y b) = (0, \pm \frac{2\pi}{3})} (k_y \mp \frac{2\pi}{3b}) \quad (2.37)$$

$$h(\vec{k}) \approx k_x \left( \frac{3ia_0\gamma_0}{2} \right) + \beta_y \left( \frac{\pm 3a_0\gamma_0}{2} \right), \text{ where } \beta_y = (k_y \mp \frac{2\pi}{3b})$$

$$h(\vec{k}) \approx \frac{i3a_0\gamma_0}{2} (k_x \mp i\beta_y) \quad (2.38)$$

Where  $h(\vec{k}) = 0$  at the Dirac points is used.

The eigenvalue  $E = |h(\vec{k})| = \sqrt{h(\vec{k}) h(\vec{k})^*}$  is given as:

$$E(\vec{k}) = \pm \frac{3a_0\gamma_0}{2} \sqrt{k_x^2 + \beta_y^2} \quad (2.39)$$

The above relation represents the equation of circles around the center points  $(0, 2\pi/3b)$  or  $(0, -2\pi/3b)$  (S. Datta, 2005) [12].

The energy dispersion relation given in Eq. 2.39 can be expressed as:

$$E(\vec{k}) = \pm \frac{3a_0\gamma_0}{2} |\vec{k}|, \text{ where } |\vec{k}| = \sqrt{k_x^2 + \beta_y^2} \quad (2.40)$$

Finally, the dispersion relation in Eq. 2.40 can be rewritten in terms of the Fermi velocity as:

$$E = \pm \hbar v_f |\vec{k}| \quad (2.41)$$

$$\text{where } v_f = \frac{1}{\hbar} \frac{dE}{dk} = \frac{1}{\hbar} \frac{3a_0\gamma_0}{2} \approx \frac{10^6 m}{s} = \frac{1}{300} c, \quad (2.42)$$

where  $c$  is the speed of light.

The linear behavior of the energy close to the Dirac points is similar to the Dirac spectrum for massless fermions (Y. Zhu et al., 2010) [10].

From the results given by Eq. 2.39 and Eq. 2.41 we can conclude the conical shape of the dispersion relation of graphene near the Dirac points as shown in Fig. 2.6.

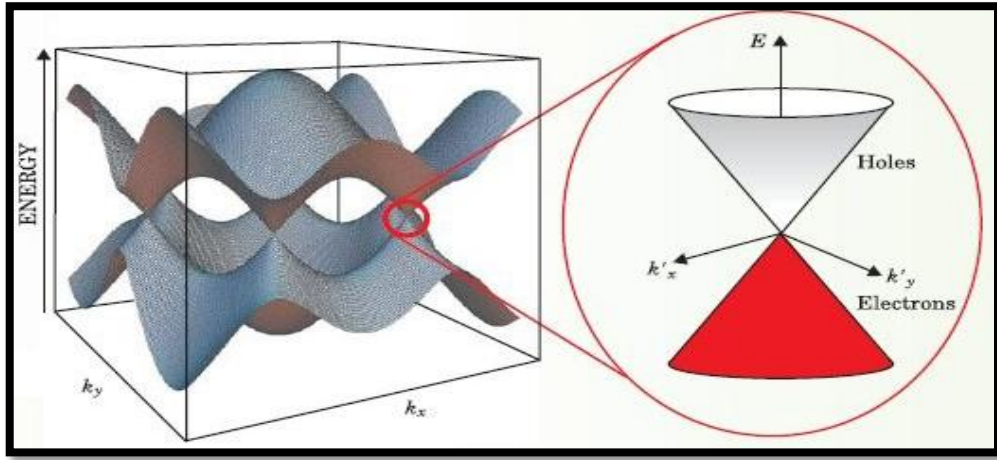


**Fig. 2.6:** The focus on the Dirac points in the dispersion relation of the graphene which show a conical shape (Jean-Noel Fuchs, 2012) [33].

## 2.7 Massless Dirac Particles:

The properties of the charge carriers of monolayer graphene at low energies are predicted to be governed by the Dirac Hamiltonian  $H_D = c\vec{\sigma} \cdot \vec{p}$  (Nan Gu, 2011) [34].

To achieve this result, we are going to present in this section the complete analytical steps which lead to the Dirac Hamiltonian of this charge carriers as follows:

Near the K point  $(0, 2\pi/3b)$  (upper half), at which  $k = K + \delta K$

where  $\delta K \ll 1$ .

$$k_x = \delta K_x \quad (2.43)$$

$$k_y = \frac{2\pi}{3b} + \delta K_y = \frac{4\pi}{3a} + \delta K_y \quad (2.44)$$

Substitute equations 2.43 and 2.44 in equation 2.35 to get:

$$h(\vec{k}) = \gamma_0 \left[ e^{-\frac{ik_x a}{\sqrt{3}}} + 2e^{\frac{ik_x a}{2\sqrt{3}}} \cos\left(\frac{k_y a}{2}\right) \right] = \gamma_0 \left[ e^{-\frac{i\delta k_x a}{\sqrt{3}}} + 2e^{\frac{i\delta k_x a}{2\sqrt{3}}} \cos\left(\left(\frac{4\pi}{3a} + \delta K_y\right)a/2\right) \right]$$

By using the well-known Taylor expansion ( $e^x = 1 + x + \dots$ ) to expand the exponential and cosine terms around  $k_x$  and  $k_y$  as:

$$\begin{aligned} h(\vec{k}) &= \gamma_0 \left[ \left(1 - \frac{i\delta k_x a}{\sqrt{3}}\right) + 2\left(1 + \frac{i\delta k_x a}{2\sqrt{3}}\right) \left(-\frac{1}{2} - \frac{\sqrt{3}}{2} \delta K_y \frac{a}{2}\right) \right] \\ &= \frac{\gamma_0 a \sqrt{3}}{2} (-i\delta k_x - \delta k_y) = \frac{\gamma_0 a \sqrt{3}}{2} (\delta k_x - i\delta k_y) \end{aligned} \quad (2.45)$$

Eq. 2.45 can be rewritten in terms of  $v_f$  as:

$$h(\vec{k}) = \hbar v_f (\delta k_x - i\delta k_y) \quad (2.46)$$

The Hamiltonian of the graphene derived in Eq. 2.46 can be written in a matrix form as:

$$H = \begin{pmatrix} 0 & h(\vec{k}) \\ h(\vec{k})^* & 0 \end{pmatrix} = \hbar v_f \begin{pmatrix} 0 & \delta k_x - i\delta k_y \\ \delta k_x + i\delta k_y & 0 \end{pmatrix} \quad (2.47)$$

We can show that the above Hamiltonian H by Eq. 2.47 can be reduced to 2D massless standard Dirac Hamiltonian  $H_D = c \vec{\sigma} \cdot \vec{p}$ , where  $\sigma$  are the well-known Pauli matrices in 2D as follow:

$$\vec{\sigma} \cdot \vec{p} = \sigma_x p_x + \sigma_y p_y, \quad \vec{p} = \hbar \delta \vec{k} \quad (2.48)$$

Using the most common representation of the Pauli matrices:

$$\sigma_x = \begin{pmatrix} 0 & 1 \\ 1 & 0 \end{pmatrix}, \quad \sigma_y = \begin{pmatrix} 0 & -i \\ i & 0 \end{pmatrix} \quad (2.49)$$

To obtain again:

$$c \vec{\sigma} \cdot \vec{p} = \hbar c [\sigma_x \delta k_x + \sigma_y \delta k_y] = \hbar c \begin{pmatrix} 0 & \delta k_x - i \delta k_y \\ \delta k_x + i \delta k_y & 0 \end{pmatrix} \quad (2.50)$$

By comparing the results obtained from equations 2.50 and 2.47 we can see that the Hamiltonian  $\hat{H}$  of graphene near  $k$  points is similar to the typical Hamiltonian  $\hat{H}_D$  of massless Dirac particles but with Fermi velocity  $v_f$ , where  $v_f = \frac{1}{300} c = 10^6 \frac{m}{s}$ .

## 2.8 Band Structure of CNTs:

For calculating electronic band structure in carbon nanotubes we will take the graphene electronic states and to account for the periodic boundary conditions in the circumferential direction. As we found that the nanotube states are the same as the set of graphene state in directions in reciprocal space that satisfy quantization condition (Ana Dergan, 2010) [30] as we mentioned early in Eq. 2.15:

$$e^{i\vec{k} \cdot \vec{C}_h} = 1 \rightarrow \vec{k} \cdot \vec{C}_h = 2\pi \nu$$

For example, Eq. 2.39 for a zigzag CNTs with periodic boundary conditions  $k_y = 2\pi \nu / 2mb$  becomes:

$$E(\vec{k}) = \pm \frac{3a_0\gamma_0}{2} \sqrt{k_x^2 + k_\nu^2}, \text{ where } k_\nu = k_y - \frac{2\pi}{3b} = \frac{2\pi}{3b} \left( \frac{3\nu}{2m} - 1 \right) \quad (2.51)$$

So if  $m$  is a multiple of three then conduction will be in a zigzag CNT;  $\frac{\nu}{2m} = \frac{1}{3}$  so  $k_\nu = 0$  and  $E$  as function of  $k_x$  becomes linear. Therefore only if  $m$  is a multiple of three then conduction will be in a zigzag nanotube. But if  $m$  is not a multiple of three the nanotube is a semiconductor with energy gap. This metallic and semiconducting behavior of CNT will be discussed thoroughly in the next chapter.

For Zigzag CNTs with periodic boundary conditions  $k_y = 2\pi \cdot 3\nu/3b \cdot 2m$ , if we substitute this in Eq. 2.34 then the dispersion relation for zigzag nanotube is:

$$E = \pm \gamma_0 \left( 1 + 4\cos(k_x a)\cos\left(\frac{\pi \nu}{m}\right) + 4\cos^2\left(\frac{\pi \nu}{m}\right) \right)^{\frac{1}{2}} \quad (2.52)$$

## 2.9 Semiconducting Gap for Zigzag CNTs:

As we said that when  $(m-n)$  is not a multiple of three, we will have a semiconducting nanotube with finite energy gap  $E_g$ .

In order to derive an expression for the energy gap of a Zigzag nanotube we will reconsider its periodic boundary condition again given by Eq. 2.16 and put them in Eq. 2.51 to get:

$$E_\nu(k_x) = \pm a\gamma_0 \sqrt{k_x^2 + \left[ \frac{2\pi}{3b} \left( \frac{3\nu}{2m} - 1 \right) \right]^2} \quad (2.53)$$

The energy gap for subband  $\nu$  can be defined as the difference in energies between the positive and negative branches at  $k_x = 0$ :

$$E_{g,\nu}(k_x) = 2a\gamma_0 \frac{2\pi}{3b} \left( \frac{3\nu}{2m} - 1 \right) = 2a\gamma_0 \frac{2\pi}{2mb} \left( \nu - \frac{2m}{3} \right) \quad (2.54)$$

The above energy gap has zero value when  $(\nu - \frac{2m}{3})=0$ ;  $\nu = \frac{2m}{3}$ ,  $m$  is a multiple of three. On the other hand, if  $m$  is not a multiple of three the energy gap in Eq. 2.54 is a non- vanishing quantity given as:

$$E_g = 2a\gamma_0 \frac{2\pi}{2mb} \frac{1}{3} = \frac{4a\gamma_0}{3d} \quad (2.55)$$

Where  $d$  is the diameter of the nanotube and equals to  $2mb/\pi$  .

## 2.10 Density of States (DOS):

The density of states  $D(E)$  in the energy interval  $E$  and  $E+\Delta E$  refers to the number of quantum states per unit energy, and it clearly depends on the  $E(\vec{k})$  relationship (S. Datta, 2005) [12].

The DOS of semiconducting CNTs near  $E=0$  does vanish, but the DOS of metallic nanotube near  $E=0$  has a finite value. In addition, the DOS of Zigzag CNTs shows Van Hove singularities (Edris Faizabadi, 2011) [20] as we will see.

### 2.10.1 Density of States of Graphene:

In order to find an expression for the density of states of graphene we assume graphene is a large sheet of dimensions  $l_x$  by  $l_y$  . Therefore, the surface area of the solid is  $l_x l_y$  . All states in this structure will be separated by the distances  $2\pi/l_x$  and  $2\pi/l_y$  (k-space). So the numbers of states lie in a given k-space area ( $dA_k = dk_x dk_y = \pi k^2$ ) is equal to:

$$N(k) = \frac{dk_x dk_y}{2\pi/l_x \cdot 2\pi/l_y}$$

If we multiply by 2 to include spin degeneracy we get:

$$N(k) = \frac{2\pi k^2 S}{4\pi^2} = \frac{k^2 S}{2\pi} \quad (2.56)$$

Where S is the surface area of 2D graphite sheet and equal to  $l_x l_y$ .

But for graphene we approximated the E ( $\vec{k}$ ) relation by:  $E(\vec{k}) = \pm \frac{3a_0\gamma_0}{2} |\vec{k}|$  at  $(k_x a, k_y b) = (0, \pm \frac{2\pi}{3})$ .

The number of states N (E) is:

$$N(E) = \frac{S}{2\pi} \left( \frac{E}{\gamma_0 a} \right)^2 \quad (2.57)$$

Using the well- known definition of the density of states as the derivative of N(E) with respect to E to obtain D(E) expression as (S. Datta, 2005) [12]:

$$D(E) = \frac{\partial N(E)}{\partial E} = \frac{S}{2\pi a^2 \gamma_0^2} |E|$$

The graphite sheet has an area which is equal  $|\vec{C}_h|L = \pi dL = S$ .

Finally, the DOS for the graphene can be obtained in a closed form as:

$$D_g(E) = \frac{Ld}{a^2 \gamma_0^2} |E| \quad (2.58)$$

### 2.10.2 Density of State of Zigzag CNTs:

The energy subbands for a Zigzag nanotube from Eq. 2.53 can be written as (S. Datta, 2005) [12]:

$$E(k_x)_{ZCNT} = \pm \gamma_0 a \sqrt{k_x^2 + k_v^2} = \pm \sqrt{(\gamma_0 a k_x)^2 + E_v^2} \quad (2.59)$$

where  $k_v \equiv \frac{2\pi}{3b} (\frac{3v}{2m} - 1)$  and  $E_v \equiv \gamma_0 a k_v$ .

To account the number of states in the zigzag one dimensional carbon nanotube, we look at how many states lie in a distance  $k$  from the origin:

$$N(k_x) = \frac{2k_x}{2\pi/L_x} = \frac{Lk_x}{\pi} \quad (2.60)$$

From equations 2.59 and 2.60 we can express the number of states  $N$  as function of  $E$  as follows:

$$N(E) = \frac{L}{\pi a \gamma_0} \sqrt{E^2 - (a \gamma_0 k_v)^2} \quad (2.61)$$

Therefore, the density of states of particular subband  $\nu$  ( $D_\nu(E)$ ) is given by:

$$D_\nu(E) = \frac{\partial N(E)}{\partial E} = \frac{L}{\pi a \gamma_0} \frac{E}{\sqrt{E^2 - (a^2 \gamma_0^2 k_v^2)}} = \frac{L}{\pi a \gamma_0} \frac{E}{\sqrt{E^2 - E_v^2}} \quad (2.62)$$

$$\text{where } E_v = \gamma_0 a k_v = \frac{2\gamma_0 a}{d} (\nu - \frac{2m}{3}) \quad (2.63)$$

The total DOS can be obtained by summing overall subbands such that:  $D(E) = \sum_\nu D_\nu(E)$ . Then the total DOS of zigzag nanotube can be given as:

$$D_{ZCNT}(E) = \sum_\nu \frac{2L}{\pi a \gamma_0} \frac{E}{\sqrt{E^2 - E_v^2}} \quad (2.64)$$

The DOS for Zigzag nanotubes can be found by replacing the summation index  $\nu$  by an integral (S. Datta, 2005) [12] as follows:  $\sum_\nu \rightarrow 2 \int d\nu$

$$D_{zCNT}(E) = 2 \int d\nu \frac{2L}{\pi a \gamma_0} \frac{|E|}{\sqrt{E^2 - E_\nu^2}} \quad (2.65)$$

$$\text{with } d\nu = \frac{dE_\nu d}{2a\gamma_0}.$$

Substitute the value of  $\partial\nu$  in Eq. 2.65 to obtain a final expression for the DOS of ZCNT as:

$$D_{ZCNT}(E) = \int_0^E dE_\nu \frac{2Ld}{\pi a^2 \gamma_0^2} \frac{|E|}{\sqrt{E^2 - E_\nu^2}} = \frac{Ld|E|}{a^2 \gamma_0^2} \quad (2.66)$$

The DOS obtained for the ZCNT in Eq. 2.66 becomes identical to the DOS of a sheet of graphite given by Eq. 2.58.

# **Chapter Three**

## **Results and Discussions**

## **Results and Discussions:**

In this chapter we make use of the obtained analytical expressions to compute and to present the obtained numerical results for the graphene dispersion relation as function of  $k_x$  and  $k_y$ , Eq. 2.33, energy dispersion as function of  $k_y$ , the ZCNTs dispersion relation for different  $\nu$  and  $m$  integers, Eq. 2.52, band gap relation for semiconducting ZCNT as function of diameter, Eq. 2.55, linear DOS of graphene for different  $m$  and  $d$  values, Eq. 2.58 and the DOS for Zigzag CNT for different  $m$  values, Eq. 2.64.

### **3.1 The Energy Dispersion Relation of Graphene:**

#### **3.1.1 The Dispersion Relation as Function of $k_x$ and $k_y$ :**

The numerical values of the energy of the graphene in the dispersion relation given by Eq. 2.33 had been calculated and displayed numerically in Fig. 3.1.1 with  $E_0 = 0$ .

Our results obtained in Fig. 3.1.1 are in agreement with the standard results reported by (H. S. Philip Wong and Deji Akinwande, 2011) [4].

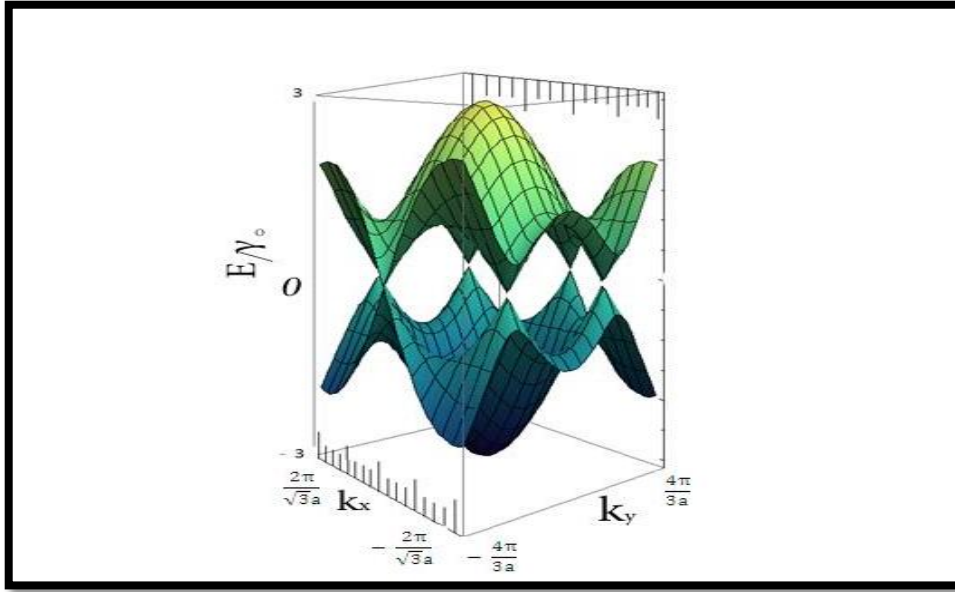


**Fig. 3.1.1:** The scaled energy as function of  $k_x$  and  $k_y$  of graphene.

### 3.1.2 The Dispersion Relation as Function of $k_y$ :

To show the behavior of the graphene near the Dirac point, we have used both the exact dispersion relation, Eq. 2.33, and the approximate results, Eq. 2.39, to obtain the numerical results of the energy against the wave vector as shown in Fig. 3.1.2. The Figure clearly shows the linear behavior of the dispersion relation close to the Dirac points.

Fig. 3.1.2 displays our calculated results against the standard results reported in (S. Datta, 2005) [12].

Fig. 3.1.2a is in agreement with one that reported in (S. Datta, 2005) [12]. However, Fig. 3.1.2.b shows the same physical equations but calculated for extended range of  $k_y b$ .

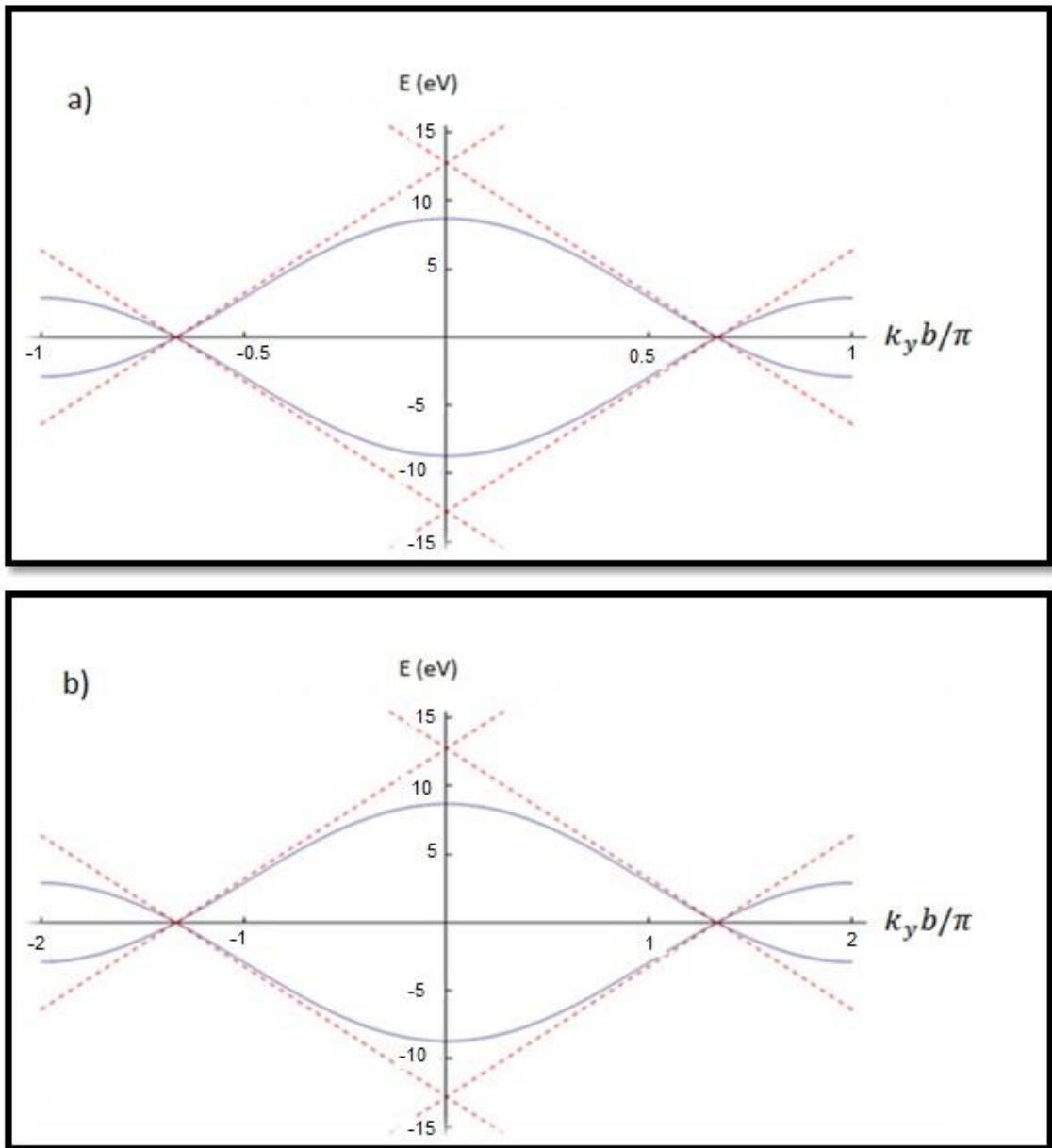


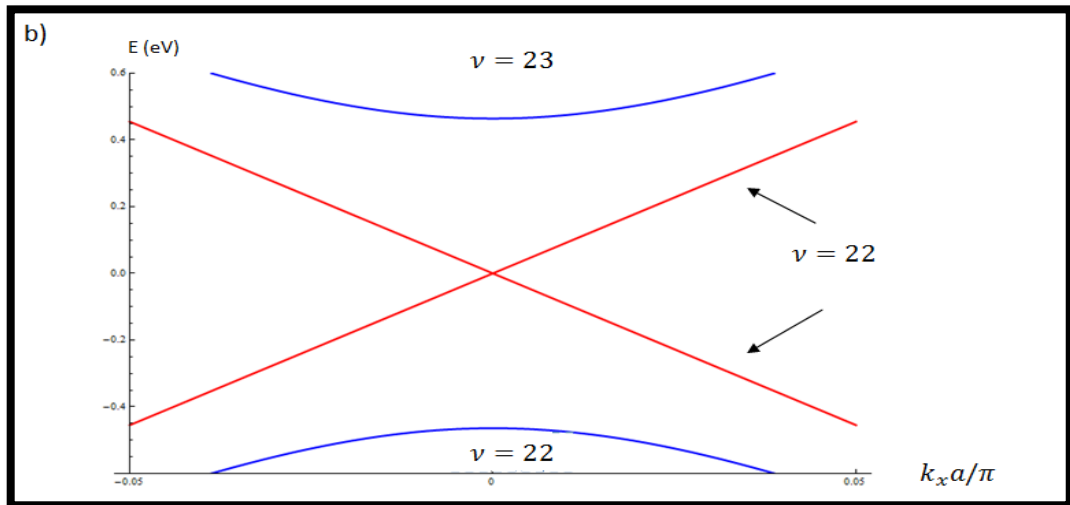
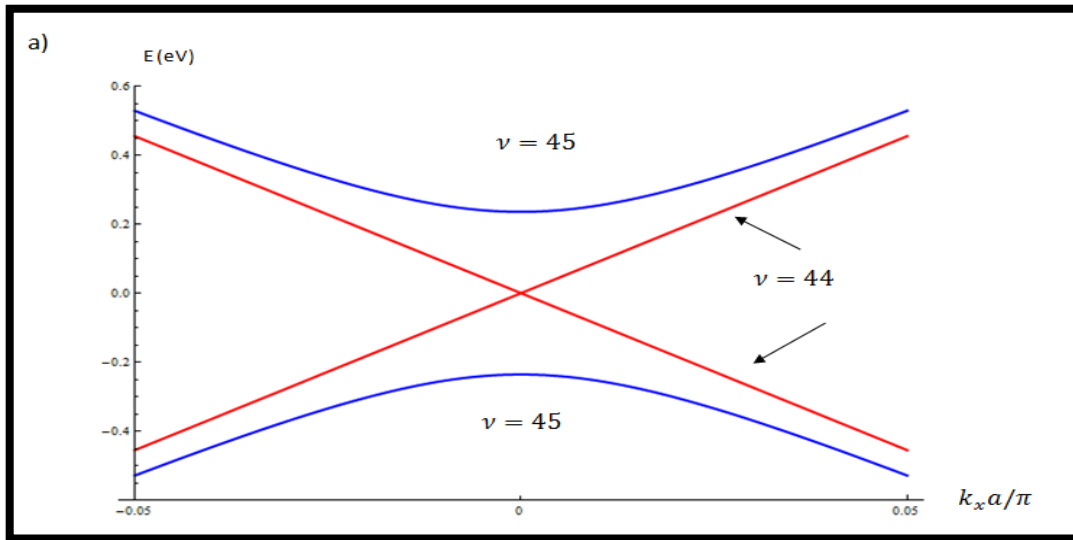
**Fig. 3.1.2:** The energy (in eV) of the graphene for arbitrary  $k_y$  values and particular restricted  $k_x$  values ( $k_x a = 0$ ). The dashed curve represents the behavior of the dispersion relation near the Dirac points Eq. 2.39, while the solid line represents the behavior of the exact dispersion relation Eq. 2.33. a) Our results compared against the standard ones (S. Datta, 2005) [12]. b) Our results calculated for extended  $k_y b$  range.

### 3.2 The Dispersion Relation for the Zigzag CNTs:

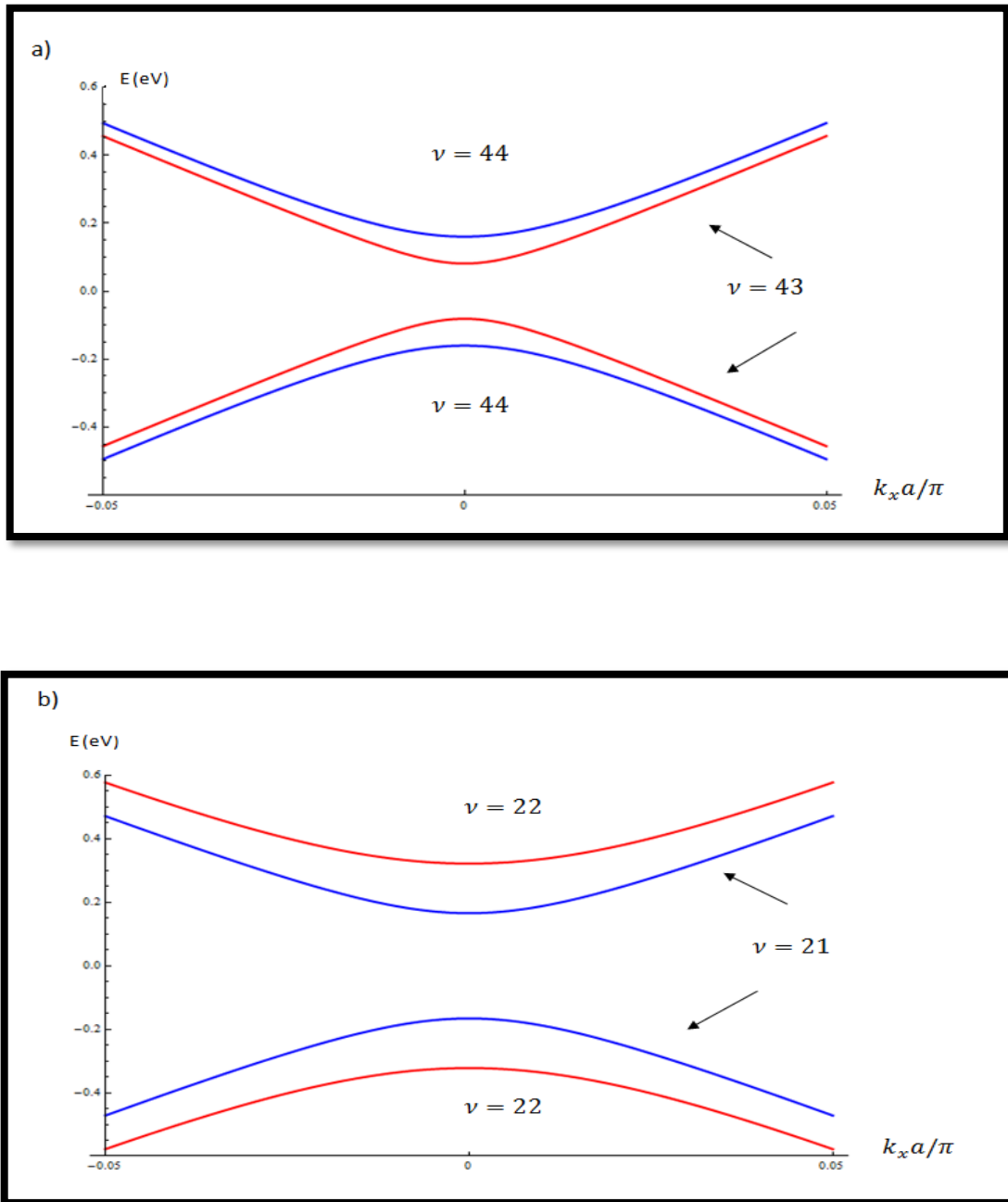
We have used the analytical dispersion relation derived for the zigzag carbon nanotubes, Eq. 2.52, to obtain the numerical energies as function of  $k_x$  for different values of  $\nu$  and  $m$  as shown in Fig. 3.2.1 and Fig. 3.2.2.

Fig. 3.2.1a and Fig. 3.2.2a are plotted to compare our results against the reported ones in (S. Datta, 2005) [12]. In Fig. 3.2.1b and Fig. 3.2.2b we have extended our calculations to consider different values of  $m$  and  $\nu$ .

Fig. 3.2.1 clearly shows that when  $m$  is a multiple of three while the band index  $\nu$  changes, the nanotube shows a metallic behavior. However, when  $m$  is not a multiple of three as in Fig. 3.2.2 a semiconducting behavior of the nanotube with a finite band gap is found.



**Fig. 3.2.1:** The eigen energies of a zigzag nanotube against the wave vector  $k_x$  for  $m$  and different  $\nu$  values showing metallic character (zero gap). a) our results with  $m=66$  compared with ones reported in (S. Datta, 2005) [12]. b) our results calculated for extended  $\nu$  values and  $m=33$ .



**Fig. 3.2.2:** The eigen energies of a zigzag nanotube versus the wave vector  $k_x$  for  $m$  and different  $\nu$  values showing semiconducting character (finite energy gap). a) our results for  $m=65$  compared with ones reported in (S. Datta, 2005) [12]. b) our results calculated for extended  $\nu$  values and  $m=32$ .

### **3.3 Semi Conducting Gap for Zigzag CNTs:**

In Fig. 3.3 we have used the closed expression that we have produced for the band gap of the zigzag carbon nanotubes given by Eq. 2.55 to calculate the the numerical values of  $E_g$  as function of the nanotube diameter.

The energy gap in Fig 3.3a shows a qualitative agreement with the corresponding ones reported in (H. S. Philip Wong and Deji Akinwande, 2011) [4].

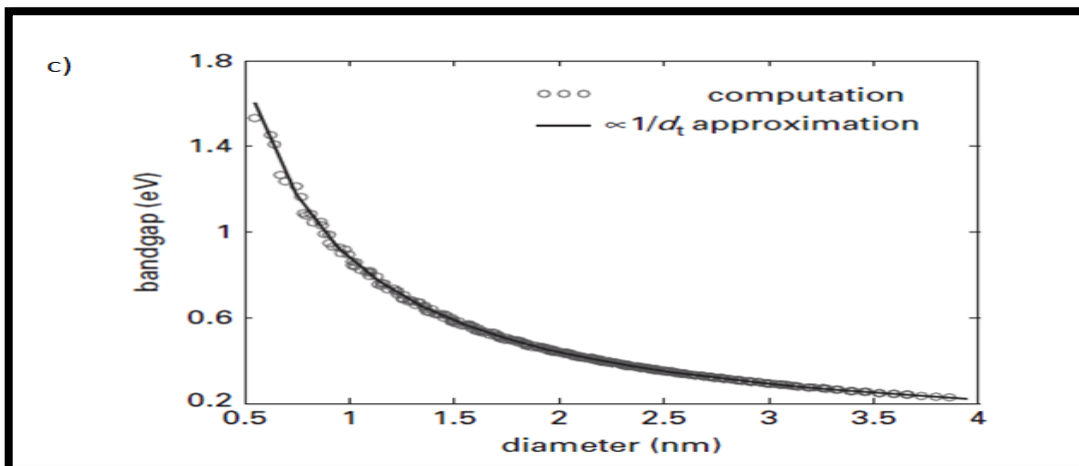
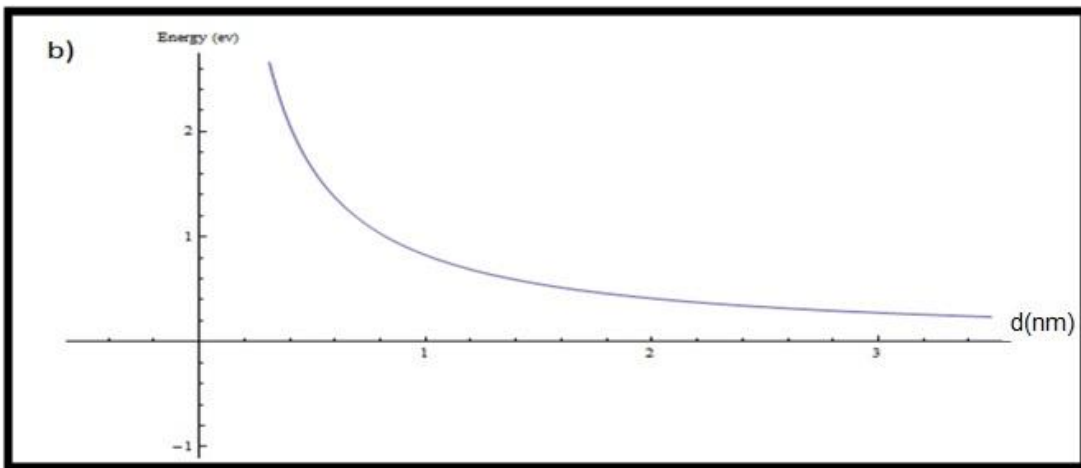
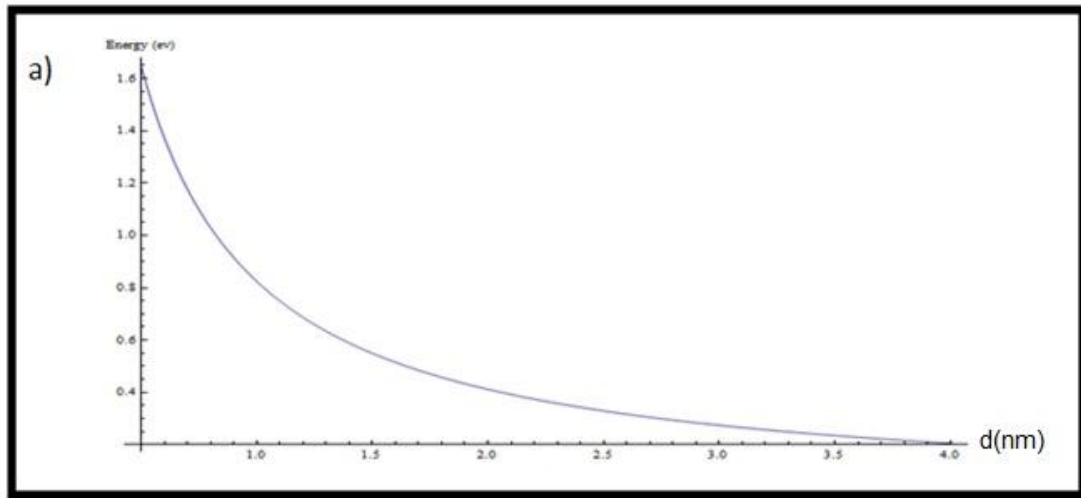


**Fig. 3.3:** The bandgap in (eV) of semiconducting Zigzag CNTs for different ranges of the diameter. a) Our results against the reported one in (H. S. Philip Wong and Deji Akinwande, 2011) [4]. b) Our numerical results for different range of the diameter. c) The band gap calculated using Eq. 2.55 (solid line) compared with exact computation showing good agreement (H. S. Philip Wong and Deji Akinwande, 2011) [4].

### **3.4 The Density of States (DOS):**

#### **3.4.1 Density of states of Graphene:**

We have used the density of states of graphene  $D_g(E)$  that produced in Eq. 2.58 to numerically display the graphene DOS against the energy  $E$  for different values of  $m$  and  $d$ .

Fig. 3.4.1 shows the linear DOS of graphene with respect to  $E$  for different  $m$  and  $d$  values ( $m=200$ ,  $d=15.4\text{nm}$ ), ( $m=900$ ,  $d=61.7\text{nm}$ ) and ( $m=400$ ,  $d=20\text{nm}$ ) and it show that at the Fermi energy ( $E_f = 0$ ) the DOS is zero.

Fig. 3.4.1a is in agreement with one that reported in (S. Datta, 2005) [12], but Fig. 3.4.1b and Fig. 3.4.1c is our results for different  $m$  and  $d$  values.

The numerical values of  $D(E)$  and  $E$  are listed in the Appendix.

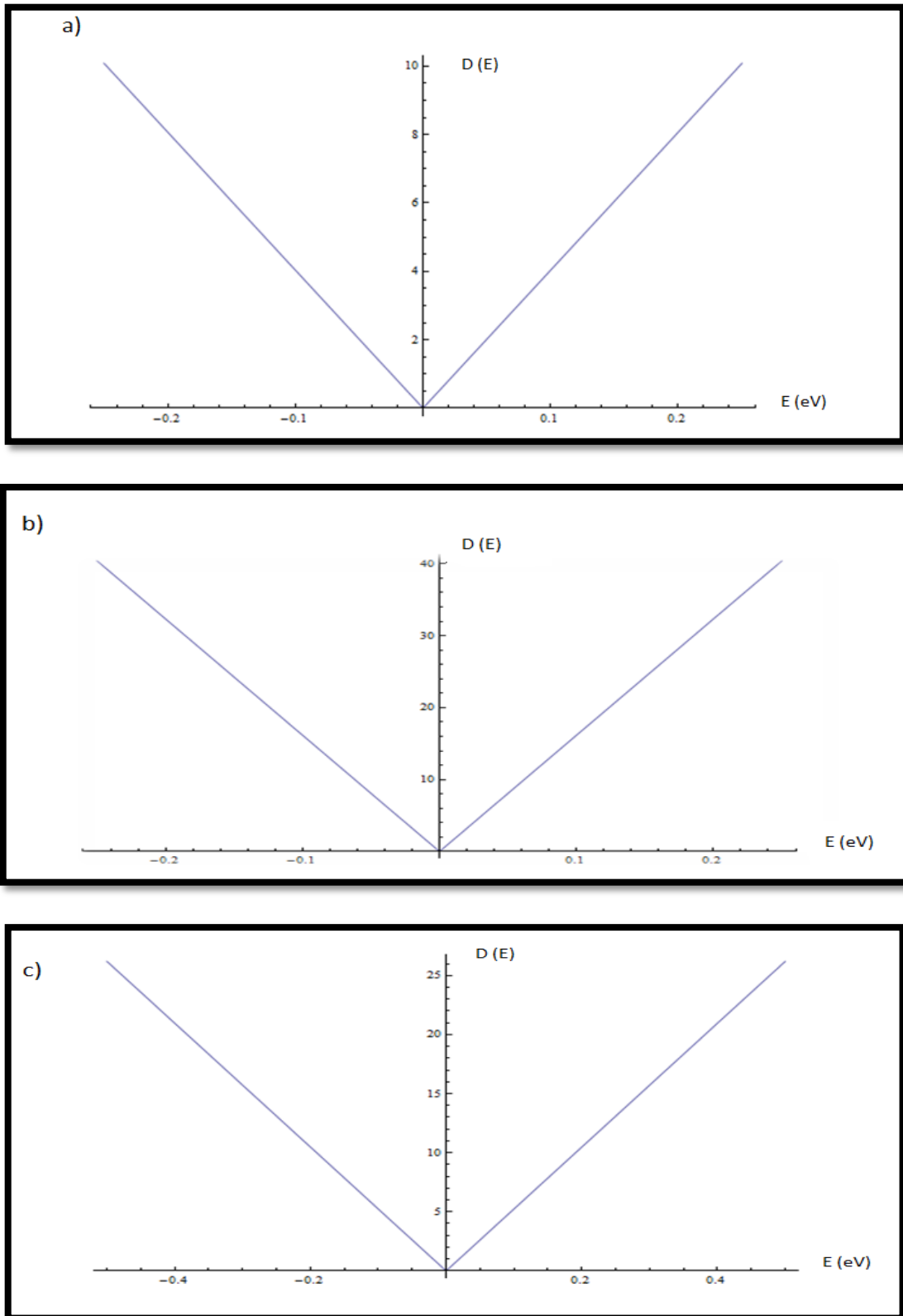


**Fig. 3.4.1:** The linear behavior of the DOS of graphene for different  $m$  and  $d$  values. a) Our results (for  $m=200$ ,  $d=15.4$  nm) compared with one reported in (S. Datta, 2005) [12]. b) Our results calculated for (for  $m=900$ ,  $d=61.7$ nm). c) Our results for (for  $m=400$ ,  $d=20$ nm).

### 3.4.2 The DOS of Zigzag CNT:

The density of states expression for Zigzag CNT derived in Eq. 2.64 had been used to calculate and display the numerical values of  $D(E)$  as a function of the energy  $E$  for different values of  $m$  for a zigzag CNT.

For example, Fig. 3.4.2a shows the DOS against  $E$  for zigzag CNT with  $m=300$  and  $d=15.4\text{nm}$ . In Fig. 3.4.3a we have plotted the same physical quantity but calculated for  $m=200$ . Our numerical results show good agreement with ones reported in (Ji-Yong Park, 2009) [11] Fig.3.4.2b and Fig. 3.4.3c. The experimental results for the DOS of semiconducting (SWCNT) are shown in Fig. 3.4.3b and it supports our numerical results in Fig. 3.4.3a.

Fig. 3.4.2 and Fig. 3.4.3 show the metallic and the semiconducting behavior of the CNT respectively. To further confirm this very important behavior, we have listed a Table for the values of  $D(E)$  and  $E$  in the Appendix to show the exact vanishing and non- vanishing of the DOS of CNT.

For example, the Table clearly shows the values of the DOS which are exactly equal to zero for energy range  $E= -0.025$  to  $E= 0.025$  for  $m=200$  and  $d=15.4\text{nm}$ , which leads to semiconducting CNT. On the other hand, the Table shows the finite values of the DOS for the same energy range when  $m$  and  $d$  are taken to be equal to  $m=300$  and  $d=15.4\text{nm}$ .

In addition, the density of state of Zigzag and armchair CNTs shows Van Hove singularities (Edris Faizabadi, 2011) [20]. And because of the singularities of DOS, high optical absorption is expected when the photon energy matches the energy separation between an occupied peak in the electron DOS and one that empty (Sandra D. M. Brown, 2000) [28].

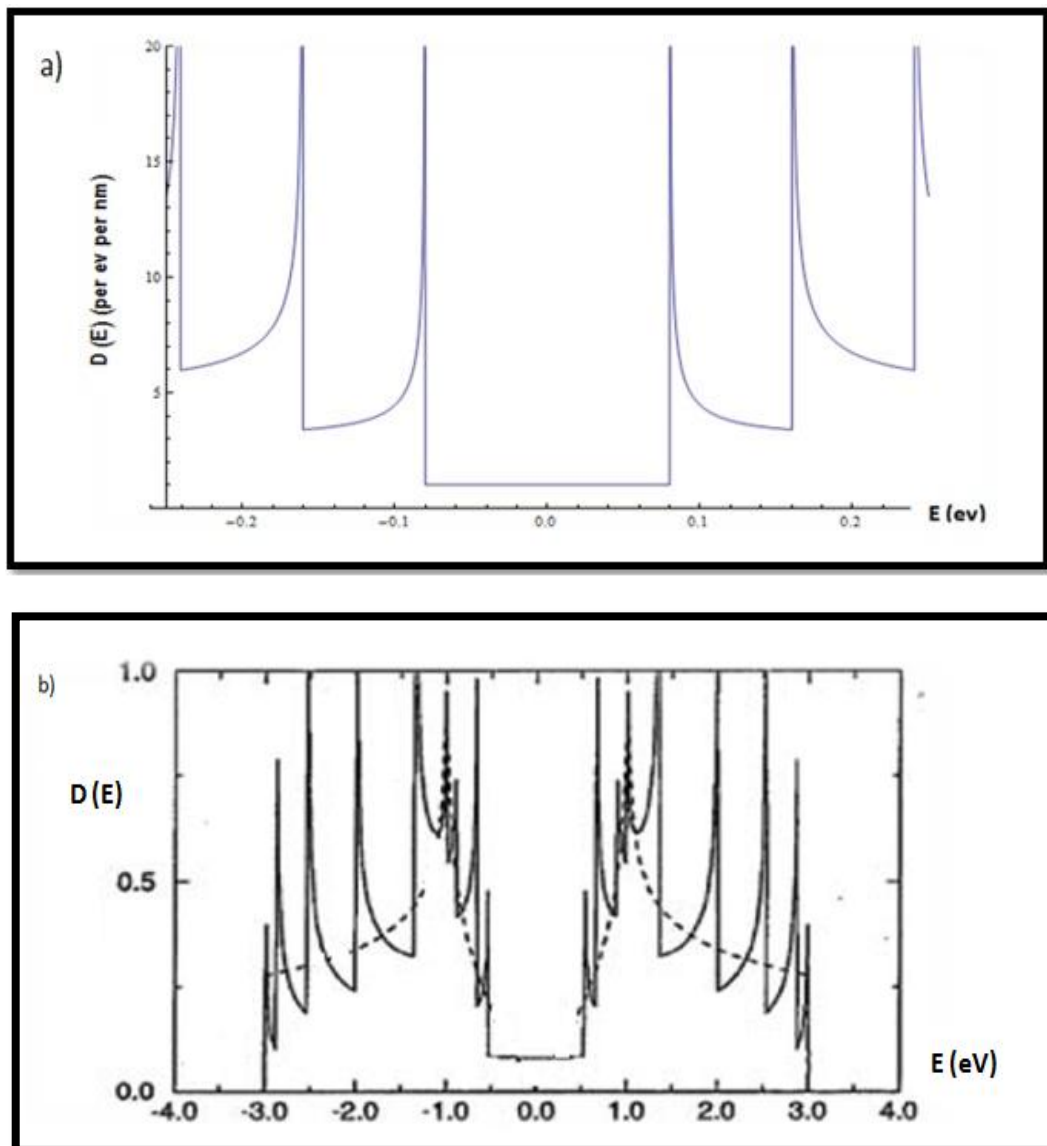


**Fig. 3.4.2:** DOS for a metallic zigzag nanotube against the energy  $E$ . a) our numerical results with  $m=300$ ,  $d=15.4$  nm. b) Results reported in (Ji-Yong Park, 2009) [11] with  $m=9$ .

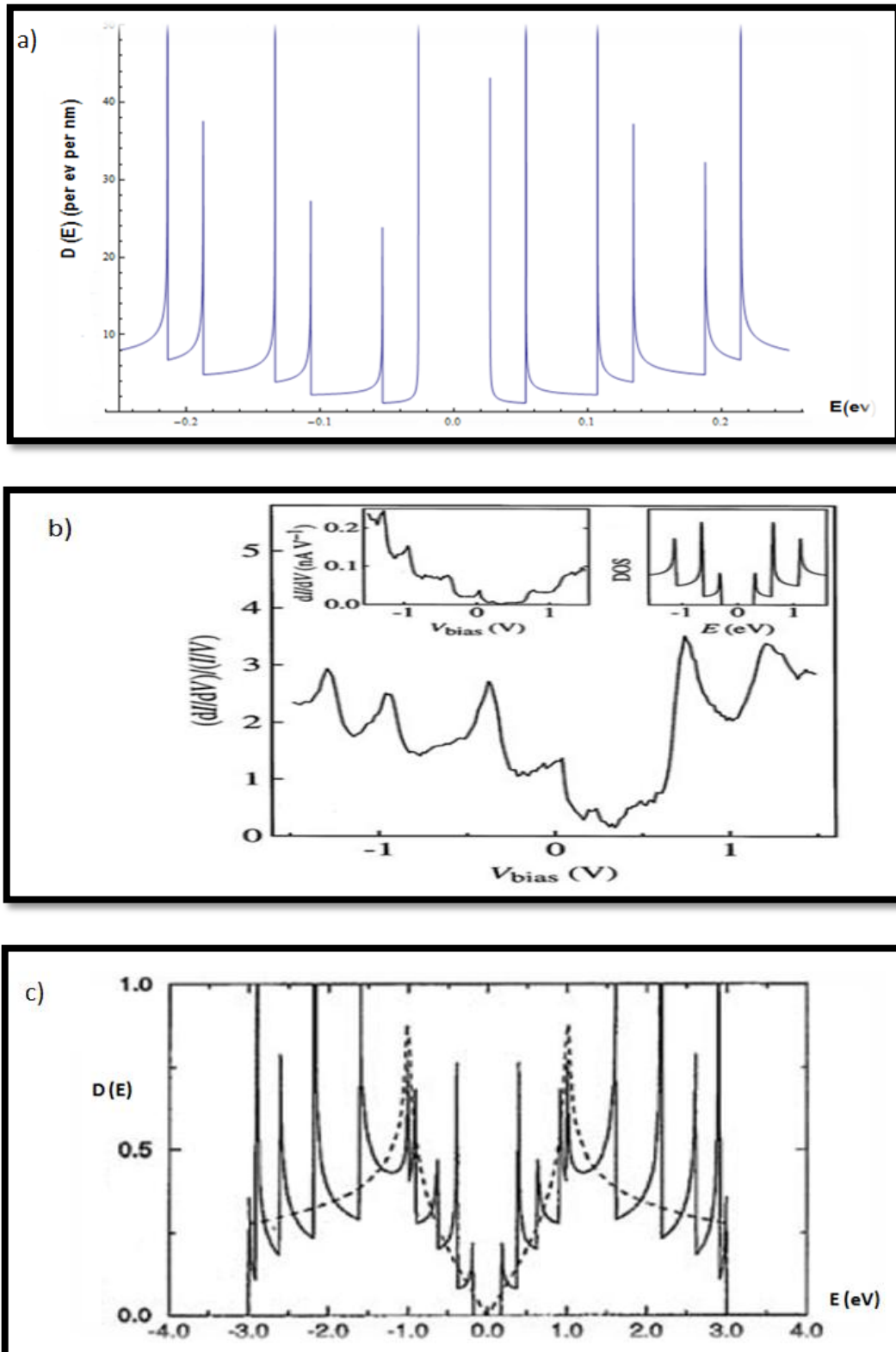


**Fig. 3.4.3:** DOS for a semiconducting zigzag nanotube against the energy  $E$ . a) our numerical result with  $m=200$ ,  $d=15.4$  nm. b) Experimental results reported in (Ji-Yong Park, 2009) [11]. c) Results reported in (Ji-Yong Park, 2009) [11] with  $m=10$ .

# **Chapter Four**

## **Conclusions**

## Conclusion:

In this thesis, we have presented a detailed study of the electronic properties of the graphene and ZCNT band structure by calculating the dispersion relation, the density of states, and the energy band gap of both graphene and ZCNT. In particular, the behavior of the particles near the Fermi Dirac points is also studied in details and its relativistic Hamiltonian found to show that the particles behave like a massless Dirac particles but with velocity  $v_f \approx c/300$ .

We have shown explicitly our numerical results for the dispersion relation, energy gap and the density of state of graphene and ZCNT.

The Figures 3.2.1, 3.2.2, 3.4.2 and 3.4.3 clearly showed the conducting and semiconducting behavior of CNT for different values of  $\nu$  and  $m$ . For example, when  $m$  is a multiple of three as in Figures 3.4.2 and 3.2.1 the metallic behavior of the CNT appeared with zero energy gaps in the dispersion relation and finite DOS at  $E = 0$ . On the other hand, if  $m$  is not a multiple of three Figures 3.2.2 and 3.4.3 the semiconducting behavior of the CNT noted with energy gap and vanishing DOS at  $E = 0$ .

The dependence of the energy gap ( $E_g$ ) of the CNT on its diameter is also calculated and displayed in Fig. 3.3 which showed an inverse relation between the energy gap and the diameter of the carbon nanotube.

Our results for the dispersion relation, Eq. 2.33, are in exact agreement with results reported in the literature (Y. Zhu et al., 2010) [10], also the DOS Eq. 2.64 and  $E_g$  Eq. 2.55 are in qualitative agreement with results reported in the literature (Rashid Nizam et al., 2011) [27]. The relativistic behavior of the Dirac particle near Dirac points  $k$  and  $k'$  in CNT also had been derived and it is found to be in agreement with (A. K. Geim et al., 2007 [7] and M. F. Craciun et al., 2011 [32]).

The attractive practical properties of graphene have encouraged both researchers and companies to use this material in several industrial fields. For example, researchers at Rice University have developed electrodes made from carbon nanotubes grown on graphene. These electrodes have a very high surface area and very low electrical resistance. Also researchers have built a solar cell that uses graphene as electrodes while using buckyballs and carbon nanotubes to absorb light and generate electrons. The intention is to eliminate the need for higher cost materials, and complicated manufacturing techniques needed for conventional solar cells ([www.Understandingnano.com](http://www.Understandingnano.com)) [35].

Processing silicon-based solar cell requires a lot of steps. But our entire device can be built using simple coating methods that don't require expensive tools and machines. The experimental solar cell consists of a layer, which absorbs sun light, sandwiched between two electrodes. In a typical thin film solar cell, the electrodes are made of conductive metals and Indium thin oxide. Materials like Indium are scarce and becoming more

expensive as the demand for solar cells, touch screen and other electronic devices. Carbon, on the other hand is low cost and earth abundant. The ability to built high frequency transistors with graphene is possible because of the higher speed at which electrons in graphene move compared to electrons in silicon. Researchers have found that graphene can replace Indium-based electrodes in organic light emitting diodes (OLED). These diodes are using in electronic device display screen which require low power consumption. The use of graphene instead of Indium not only reduces the cost but eliminates the use of metals in the (OLED), which may make devices easier to recycle ([www. Understandingnano.com](http://www.Understandingnano.com)) [35].

These interesting device applications of carbon nanomaterials will be studied in details in our future research.

## References

- [1] Andry K. Geim and Allan H. MacDonald, “**Graphene: Exploring Carbon Flatland**”, *Physics Today*, **60**, pp. 35-40, (2007).
- [2] N. M. Peres, “**Graphene: New Physics in Two Dimensions**”, *Europhysics News*, **40/3**, doi: 10.1051/epn/2009501, pp. 17-20, (2009).
- [3] Mandar M. Deshmukh and Vibhor Singh, “**Graphene- An Exciting Two- Dimensional Material for Science and Technology**”, *Resonance*, **16**, pp. 238-253, (2011).
- [4] H. S. Philip Wong and Deji Akinwande, “**Carbon Nanotube and Graphene Device Physics**”, Cambridge University Press, (2011).
- [5] Leonid Levitov, “**Graphene: Electron Properties and Transport Phenomena**”, summer school in Condensed Matter Physics, (2008).
- [6] P. Avouris, Z. Chen and V. Perebeinos, “**Carbon-Based Electronics**”, *Nature Nanotechnology*, **2**, pp. 605, (2007).
- [7] A. K. Geim and K. S. Novoselov, “**The Rise of Graphene**”, *Nature Materials*, **6**, pp. 183, March (2007).
- [8] Michael Fuhrer and Ellen Williams, “**Graphene: Massless Electrons in Flatland**”, University of Chile, (2008).
- [9] A.K. Geim, “**Graphene: Status and Prospects**”, *Science Magazine*, **324**, pp. 1530-1534, (2009).

- [10] Yanwu Zhu et al., “**Graphene and Graphene Oxide: Synthesis, Properties, and Applications**”, *Advanced Materials*, **22**, 3906-3924, (2010).
- [11] Ji-Yong Park, “**Carbon Nanotube Electronics**”, edited by Ali Javey and Jing Kong, Springer, pp. 1-42, (2009).
- [12] Supriyo Datta, “**Quantum Transport: Atom to Transistor**”, Cambridge University Press, (2005).
- [13] R. Saito, G. Dresselhaus and M. S. Dresselhaus, “**The Physical Properties of Carbon Nanotubes**”, Imperial College Press, (1998).
- [14] S. Russo. M. F. Gracium, T. Khodkov, M. Koshino, M. Yamamoto and S. Tarucha in **Carbon Nanotube Devices** edited by FrancoisL Leonard, William Andrew Inc, (2009).
- [15] [http://en.wikipedia.org/wiki/Graphene#cite\\_note-Wallace-80](http://en.wikipedia.org/wiki/Graphene#cite_note-Wallace-80)
- [16] Ron Beech, “**Nanoscale Graphene Platelets Taking Its Place as an Emerging Class of Nanomaterials**”, *Nanotechnology Law and Business*, pp. 3-6, (2011).
- [17] S. Iijima, “**Helical Microtubes of Graphitic Carbon**”, *Nature (London)*, **354**, pp. 56-58, (1991).
- [18] Paul L. McEuen, “**Single-Wall Carbon Nanotubes**”, *Physics World*, pp. 31-36, (2000).

- [19] Tara Spires and R. Malcolm Brown, “**High Resolution TEM Observations of Single-Walled Carbon Nanotubes**”, Jr. Department of Bontany, The University Of Texas at Austin Tx., 78713(1996).
- [20] Edris Faizabadi, “**Single Wall Carbon Nanotubes in the Presence of Vacancies and Related Energygaps**”, Ieran University of Science and Technology, Tehran, 603-604, July (2011).
- [21] Paul L. McEuen and Ji-Yong Park, “**Electron Transport in Single-Walled Carbon Nanotubes**”, MRS Bulletin, **29**, pp. 272-275, April (2004).
- [22] Mildred S. Dressel haus, **Fifty years in Studying Carbon-Based Materials**, Phys. Scripta **T146** 014002,pp. 1-8, (2012).
- [23] Rene Petersen, “**Tight-Binding Based Modeling of Graphene Antidot Structures**”, Aalborg University, pp. 5-13, January (2009).
- [24] Davod Fathi, “**A Review of Electronic Band Structure of Graphene and Carbon Nanotubes Using Tight Binding**”, Journal of Nanotechnology, **2011**, pp. 1-6, (2011).
- [25] Wen-Shing Jhang, “**The Synthesis and Characterization of CdSe/ZnS/CNT Nanocomposites**”, Tatung University, pp. 1-5, (2006).
- [26] Luke Anthony Kaiser Donev, “**Carbon Nanotube Transistors: capacitance Measurements, localized damage, and uses as gold scaffolding**”, Cornell University, 3-34, (2009).

- [27] Rashid Nizam, S. Mahdi A. Rizvi, Ameer Azam, “**Calculating Electronic Structure of Different Carbon Nanotubes and Its Affect on Band Gap**”, International Journal of Science and Technology, **1** (4), 153-162, (2011).
- [28] Sandra Dawn Marie Brown, “**Resonance Raman Spectroscopy of Single-Walled Carbon Nanotubes**”, Massachusetts Institute of Technology, (2000).
- [29] R. Bruce Weisman, “**Fluorescence of Single-Walled Carbon Nanotubes: Applications in Physics, Chemistry, and Bio-medicine**”, Rice University, February (2010).
- [30] Ana Dergan, “**Electronic and Transport Properties of Carbon Nanotubes**”, University of Ljubljana, pp. 2-6, October (2010).
- [31] M. P. Anantram and F. Leonard, “**Physics of Carbon Nanotube Electronic Devices**”, Institute Of Physics Publishing, **69**, pp. 507-561, (2006).
- [32] M. F. Craciun, S. Russo, M. Yamamoto and S. Tarucha”**Tuneable Electronic Properties in Graphene**”, Nano Today, **6**, pp. 42-60, 23 Jan (2011).
- [33] Jean Noel Funchs, “**Electronic Properties of Graphene**”, University Paris-Sud (Orsay), (2012).

[34] Nan Gu, “**Relativistic Dynamics and Dirac Particles in Graphene**”,  
Massachusetts Institute Of Technology, pp. 9-10, June (2011).

[35] [\*\*http://www.understandingnano.com/graphene-applications.html\*\*](http://www.understandingnano.com/graphene-applications.html).

## Appendix

The DOS of semiconducting CNT with  $m=200$  and for metallic CNT with  $m=300$ .

m=200, d=15.4 nm		m=300, d=15.4 nm	
E (eV)	D (E)	E (eV)	D (E)
-0.25	7.99797	-0.25	13.5079
-0.245	8.1801	-0.245	16.9424
-0.24	8.40679	-0.24	5.98928
-0.235	8.70092	-0.235	6.04467
-0.23	9.10757	-0.23	6.10679
-0.225	9.73477	-0.225	6.17696
-0.22	10.9546	-0.22	6.25689
-0.215	17.0071	-0.215	6.34882
-0.21	6.91244	-0.21	6.45576
-0.205	7.20225	-0.205	6.58191
-0.2	7.64098	-0.2	6.73327
-0.195	8.43724	-0.195	6.91877
-0.19	10.8188	-0.19	7.15253
-0.185	4.87249	-0.185	7.45829
-0.18	4.9423	-0.18	7.88012
-0.175	5.02482	-0.175	8.51177
-0.17	5.12408	-0.17	9.60362
-0.165	5.24618	-0.165	12.2197
-0.16	5.40096	-0.16	3.41296
-0.155	5.60561	-0.155	3.43962
-0.15	5.89403	-0.15	3.47006
-0.145	6.34699	-0.145	3.50508
-0.14	7.23762	-0.14	3.54574
-0.135	11.3113	-0.135	3.59344
-0.13	3.99722	-0.13	3.6501
-0.125	4.1869	-0.125	3.71841
-0.12	4.48196	-0.12	3.80223
-0.115	5.02969	-0.115	3.90741
-0.11	6.65702	-0.11	4.04322
-0.105	2.26339	-0.105	4.22535
-0.1	2.28929	-0.1	4.48306
-0.095	2.32105	-0.095	4.87865
-0.09	2.36078	-0.09	5.57754

m=200, d=15.4 nm		m=300, d=15.4 nm	
-0.07	2.71257	-0.07	1.03063
-0.035	1.59736	-0.035	1.03063
-0.03	2.27346	-0.03	1.03063
<b>-0.025</b>	<b>0</b>	<b>-0.025</b>	<b>1.03063</b>
<b>-0.02</b>	<b>0</b>	<b>-0.02</b>	<b>1.03063</b>
<b>-0.015</b>	<b>0</b>	<b>-0.015</b>	<b>1.03063</b>
<b>-0.01</b>	<b>0</b>	<b>-0.01</b>	<b>1.03063</b>
<b>-0.005</b>	<b>0</b>	<b>-0.005</b>	<b>1.03063</b>
<b>5.20417*10<sup>-18</sup></b>	<b>0</b>	<b>5.20417*10<sup>-18</sup></b>	<b>1.03063</b>
<b>0.005</b>	<b>0</b>	<b>0.005</b>	<b>1.03063</b>
<b>0.01</b>	<b>0</b>	<b>0.01</b>	<b>1.03063</b>
<b>0.015</b>	<b>0</b>	<b>0.015</b>	<b>1.03063</b>
<b>0.02</b>	<b>0</b>	<b>0.02</b>	<b>1.03063</b>
<b>0.025</b>	<b>0</b>	<b>0.025</b>	<b>1.03063</b>
0.03	2.27346	0.03	1.03063
0.035	1.59736	0.035	1.03063
0.04	1.3858	0.04	1.03063
0.1	2.28929	0.1	4.48306
0.105	2.26339	0.105	4.22535
0.11	6.65702	0.11	4.04322

جامعة النجاح الوطنية

كلية الدراسات العليا

## التركيب الالكتروني للغرافين وأنايبب الكربون النانوية

اعداد

أسمهان عنان سليمان ترياقى

اشراف

أ.د.محمد السعيد

د.موسى الحسن

قدمت هذه الأطروحة استكمالاً لمتطلبات الحصول على درجة الماجستير في الفيزياء بكلية الدراسات العليا في جامعة النجاح الوطنية في نابلس، فلسطين.

2013 م

ب

## التركيب الالكتروني للغرافين وأنابيب الكربون النانوية

اعداد

أسمهان عنان سليمان تريافي

اشراف

أ.د.محمد السعيد

د.موسى الحسن

### الملخص

في هذا العمل قمنا بإعادة اشتقاق علاقة لكثافة المستويات لكل من الغرافين وأنابيب الكربون النانوية باستخدام علاقة تشتت الطاقة التي تم التوصل إليها باستخدام طريقة الربط الضيق. كما وقمنا بإنتاج النتائج العددية ورسمها باستخدام برنامج الماثماتيكا لكثافة المستويات للغرافين وأنابيب الكربون النانوية والتي وضحت متى تتصرف أنابيب الكربون النانوية كموصل أو شبه موصل. كما توصلنا الى علاقة فجوة الطاقة وكذلك رسمها.

بالإضافة الى ذلك تم دراسة تصرف الجسيمات داخل الغرافين وكأنها جسيمات ديراك النسبية. وأخيرا تم مقارنة النتائج العددية التي توصلنا لها مع العديد من المقالات المنشورة وكان هناك توافق كبير بين هذه النتائج.

